



**NORTH CAROLINA AGRICULTURAL  
AND TECHNICAL STATE UNIVERSITY**

D.O.E. Project DE-FE0031747

---

## **Alloy for Enhancement of Operational Flexibility of Powerplants**

---

Ahmed C. Megri (PI)  
North Carolina A&T State University

Alireza Tabarraei (co-PI)  
UNC Charlotte

*AGGIES***DO**



## *Outline*

Heat Transfer Coefficient vs.  
Steam Mass Flow

Heat Transfer Coefficient  
vs. Pressure Drop

Steam Design Header

North Carolina A&T State University

UNC Charlotte



NORTH CAROLINA AGRICULTURAL  
AND TECHNICAL STATE UNIVERSITY

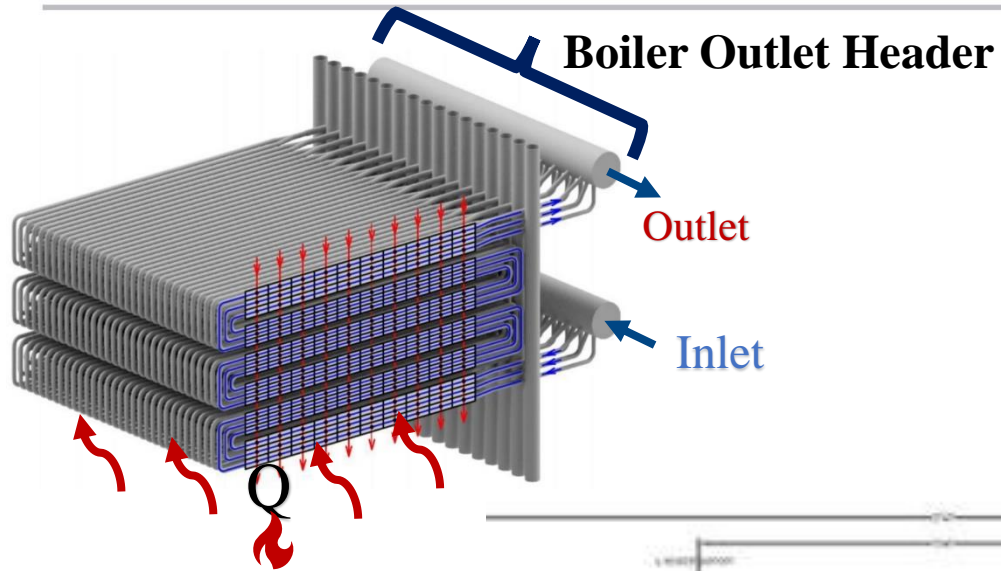
---

# *PART I: HEAT TRANSFER COEFFICIENT VS. STEAM MASS FLOW*

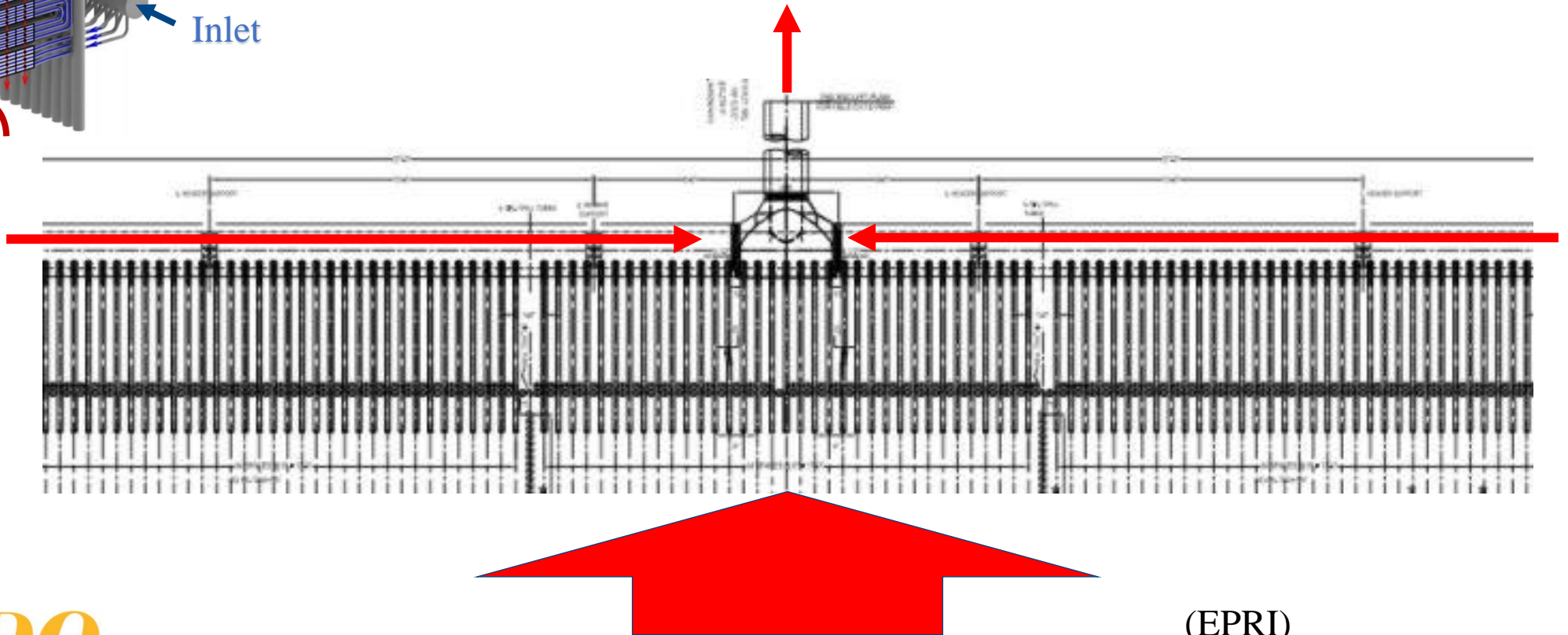
---

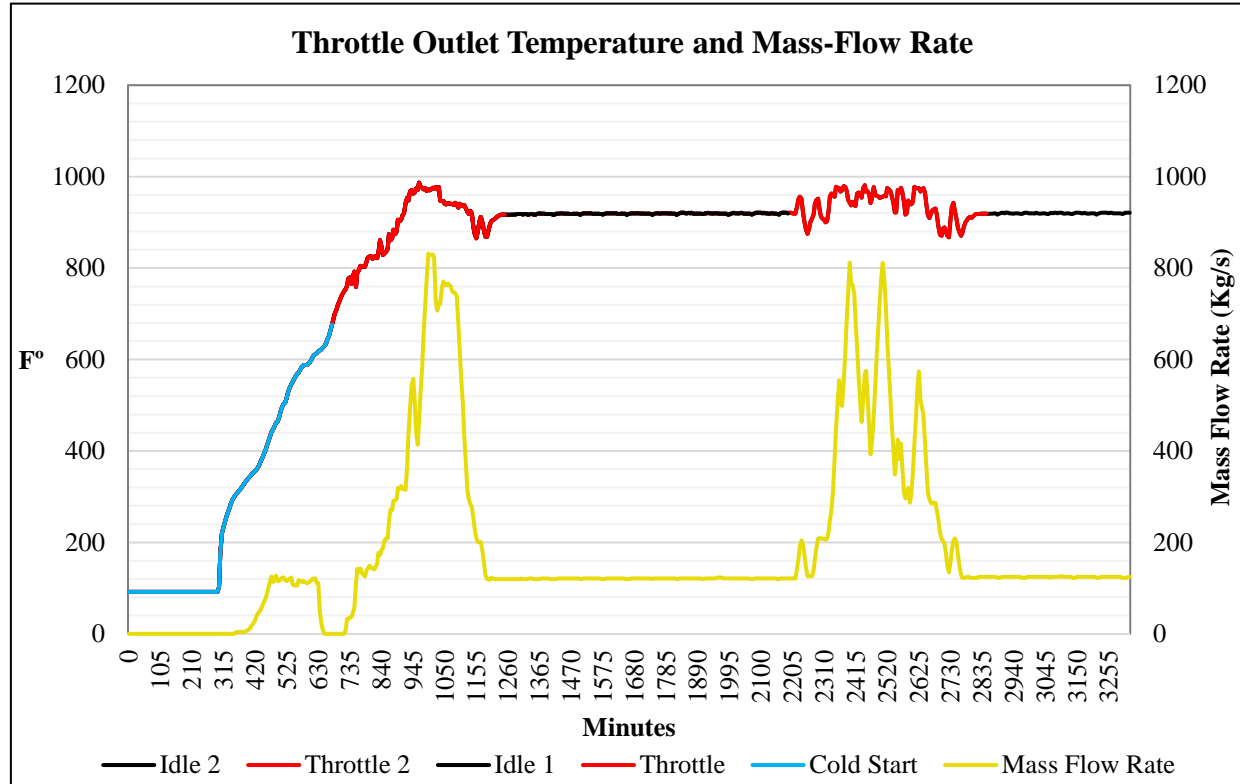
*PREDICTION OF HEAT TRANSFER COEFFICIENT USING  
MACHINE LEARNING*

AGGIES **DO**



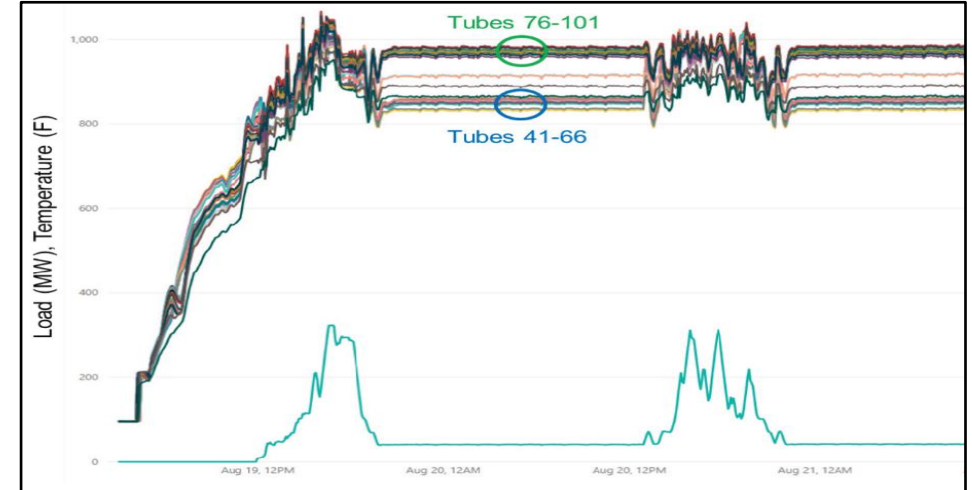
## *320MW Outlet Header*



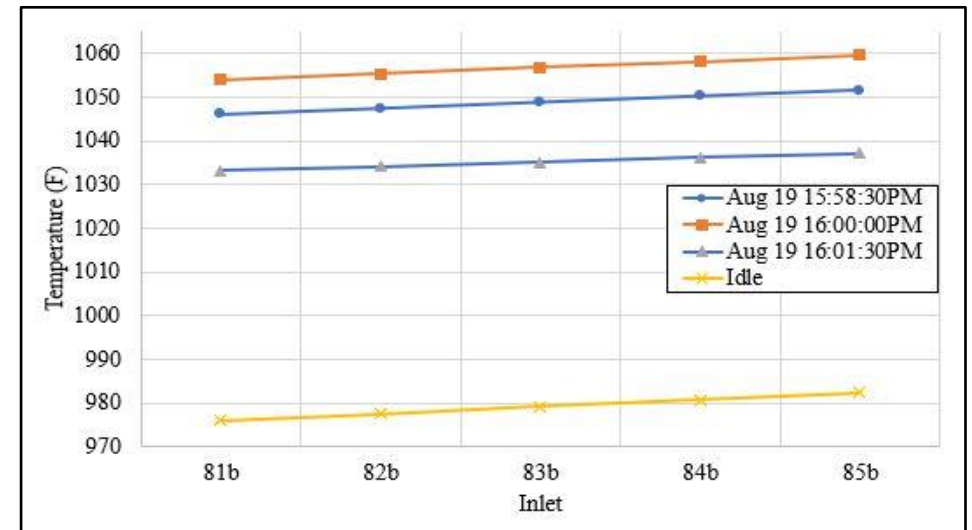


Given

- ❖ Startup cycle of a 320MW powerplant was recorded over 53 hours.
- ❖ Temperature was recorded at each branch inlet.
- ❖ Temperature and total Mass flow rate was recorded at the throttle outlet.
- ❖ Data sampling frequency: 5 minutes.



(EPRI, 2020)

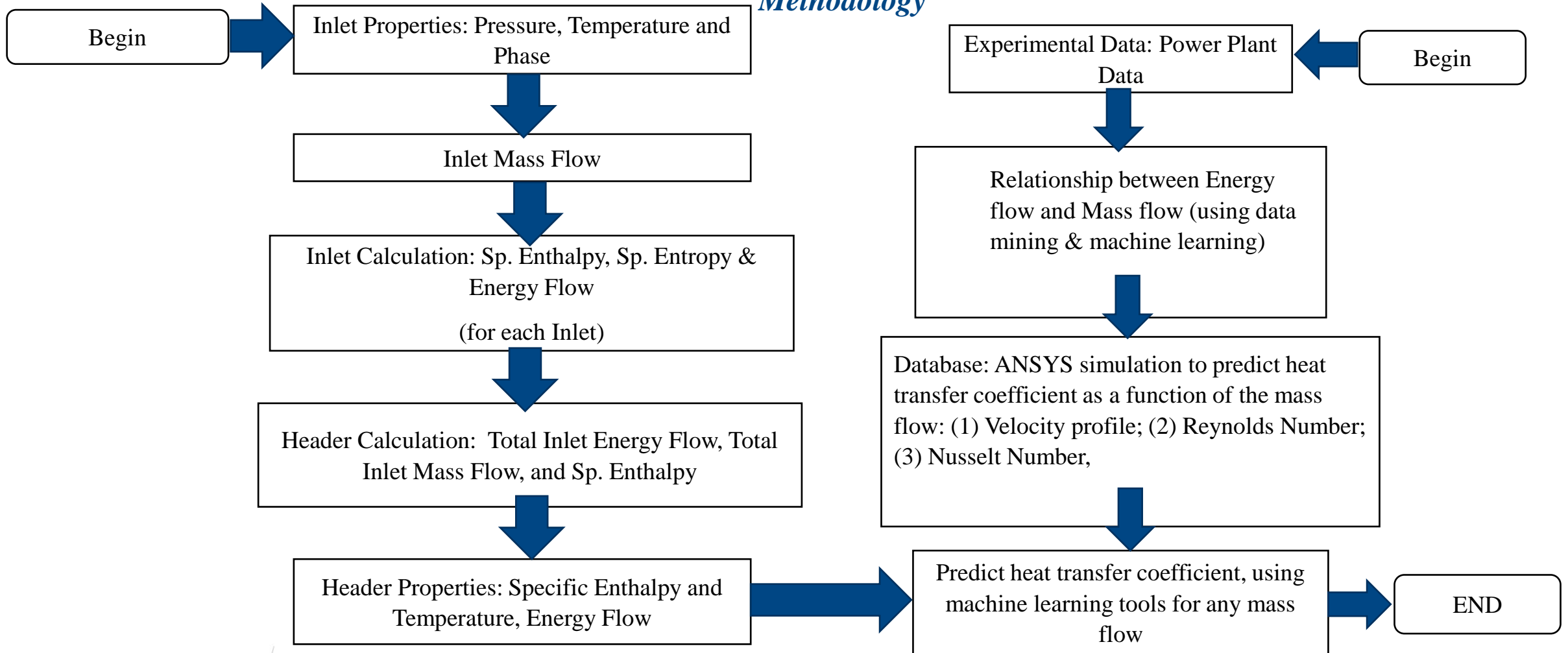


# First Set of Experimental Data

- Data from a real Power Plant
- Pressure, temperature, mass flow (no heat transfer is measured).
- Measurement over time (10 days measurement)
- Transient State ANSYS simulation



### Methodology





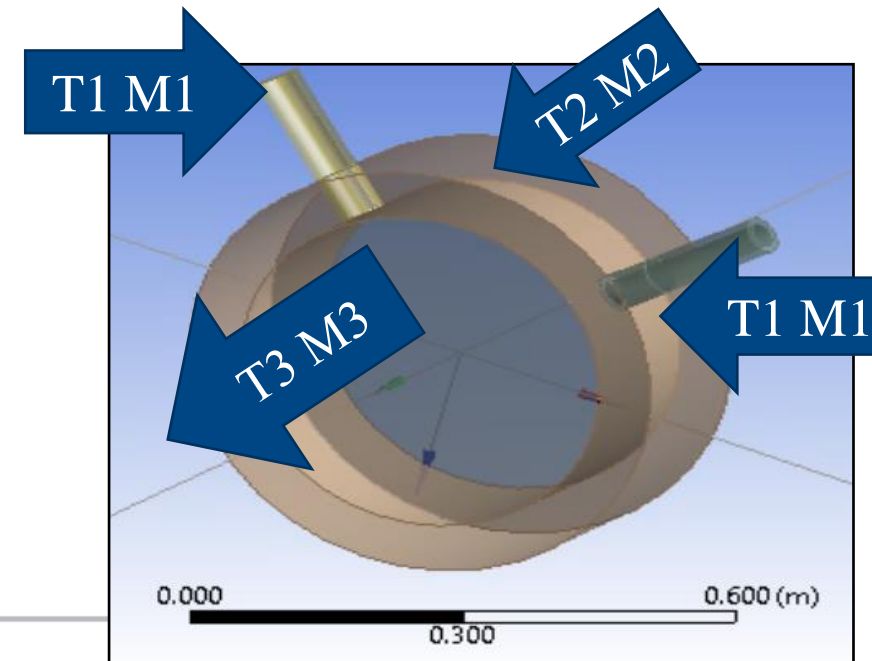
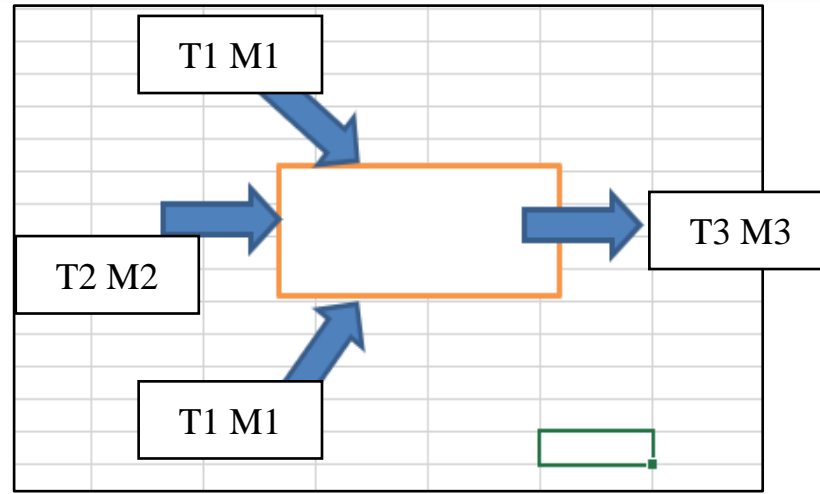
# Assumptions

- Steady-state
- Ideal Gas
  - » Using **Pressure** based formulation to calculate density from pressure and temperature .
- Reference Density
  - » Low **Mach** number flow
  - » Introduced to improve stability of the system.
- Compressible
- Operating Pressure of 1 Atm





- Input:
  - » Temperatures:  $T_1$ ,  $T_2$ ,  $T_3$
  - » Steam mass flow:  $F_1$ ,  $F_2$ ,  $F_3$
- Output:
  - » Heat Transfer Coefficient



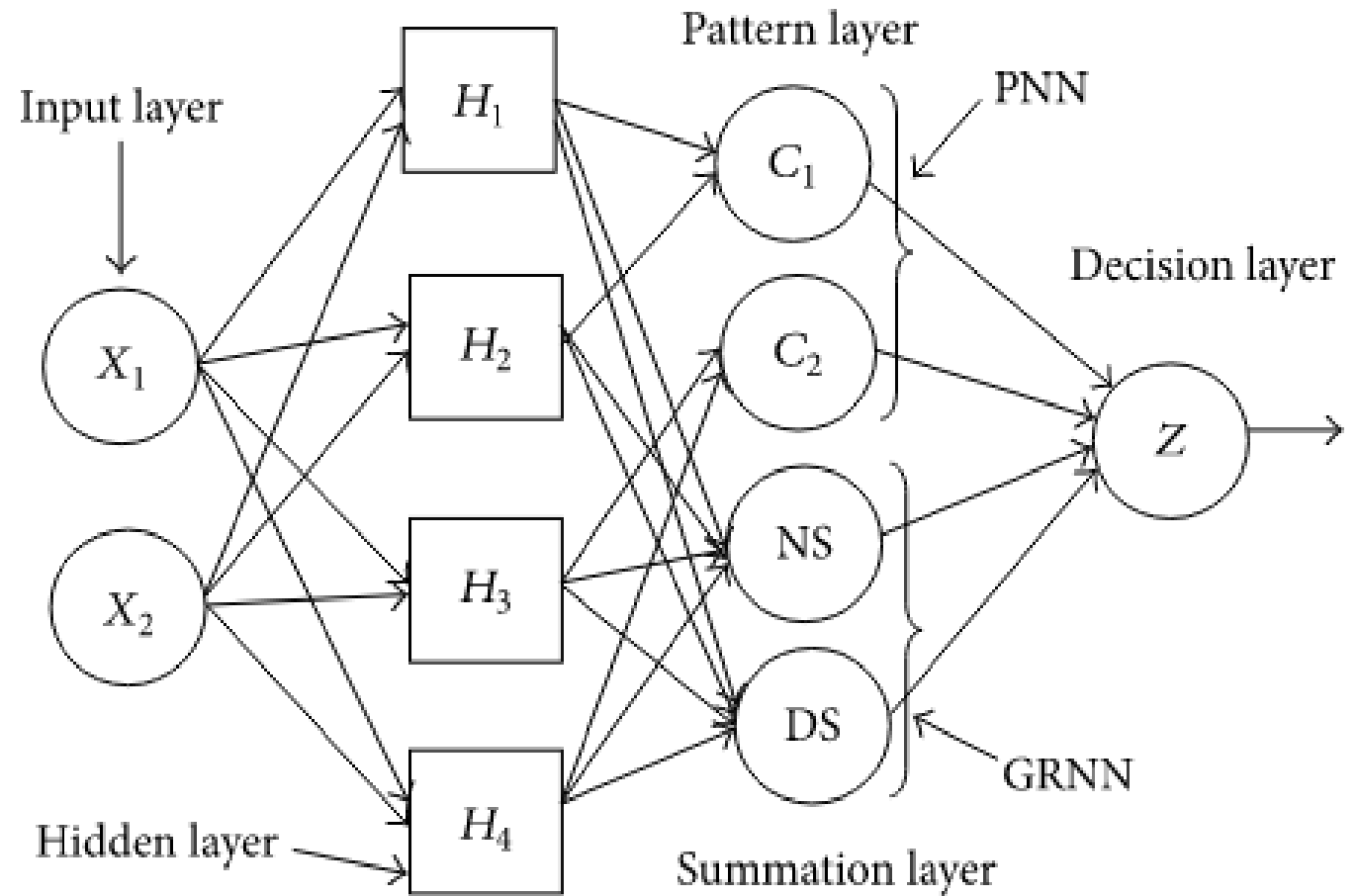
# Predictive Models

- Simulation Data (Database)
- Develop the models (70% are for training & 30% are for Testing)
- Comparison between actual vs. model
  - » (1) Prediction of Heat Transfer Coefficient as function of the main mass flow;
  - » (2) Evaluation of the models using visualization techniques (gain & lift)

## Methods

- Multilayer Perceptron
- PNN/GRNN Neural Network
- RBF Network
- GMDH Polynomial Network
- Cascade Correlation Network

## Neural Network

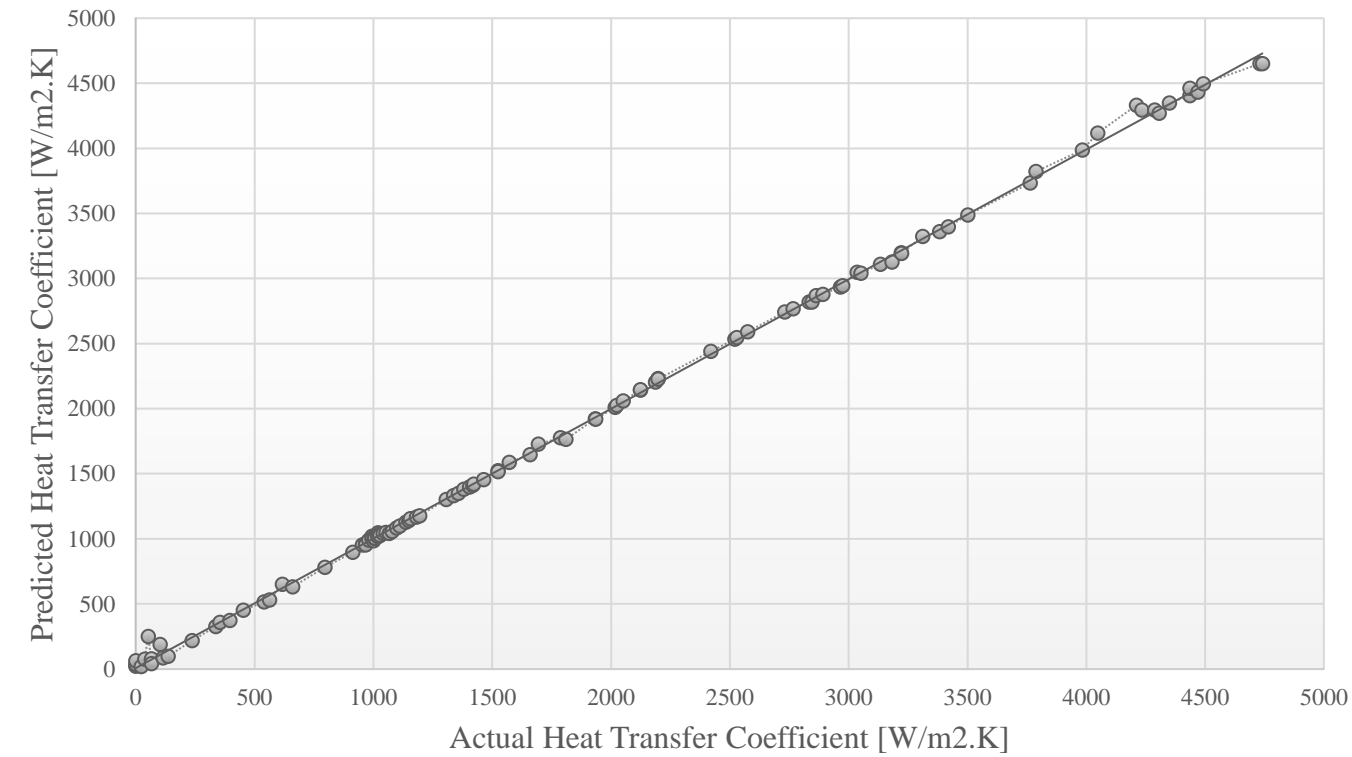




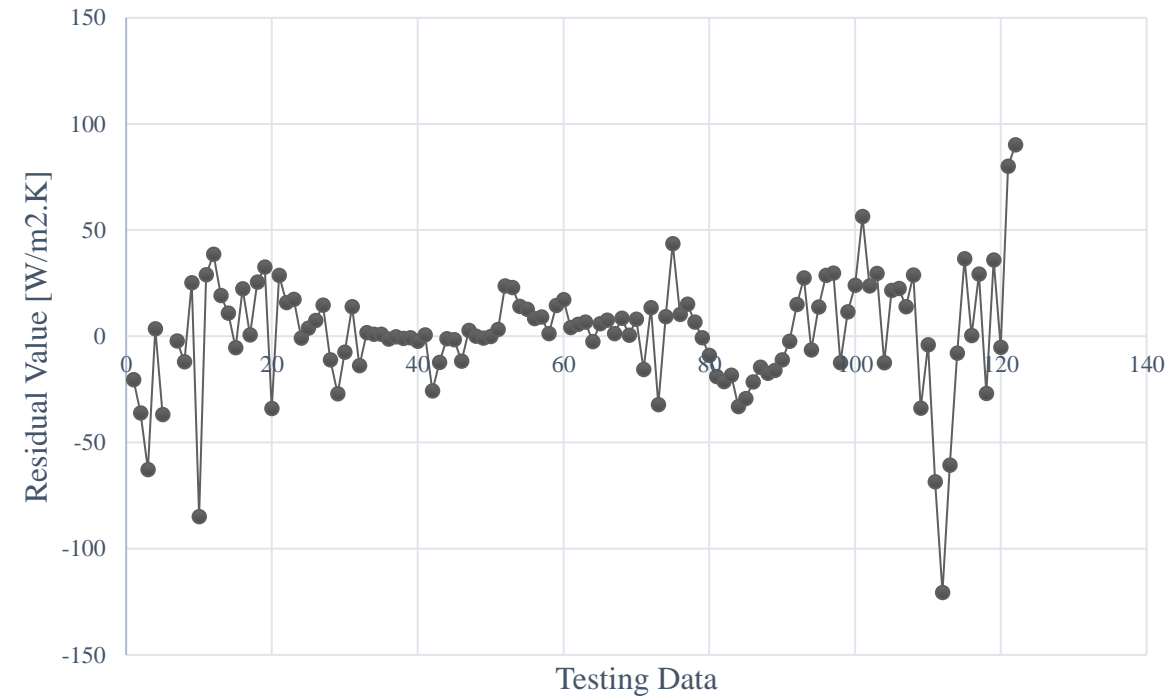
| Method                             | Number of layers | Number of Neurons | Other information related to inputs   |
|------------------------------------|------------------|-------------------|---|
| <b>Multilayer Perceptron</b>       | 3 layers         | 6, 7, 1 Neurons   | <ul style="list-style-type: none"><li>• 3 layers (1 hidden)</li><li>• Automatic hidden layer neuron selection</li><li>• Validation: Random 20%</li><li>• Hidden layer activation function: Logistic</li><li>• Output layer activation function: Logistic</li><li>• Traditional conjugate gradient</li></ul> |
| <b>PNN/GRNN Neural Network</b>     |                  | 79                | <ul style="list-style-type: none"><li>• Sigma for each variable</li><li>• Constrain minimum sigma values</li><li>• Model optimization and simplification: remove unnecessary neurons (Minimize error)</li><li>• Random: 20%</li><li>• Type of kernel function: Gaussian</li></ul>                           |
| <b>RBD Network</b>                 |                  | 9                 | <ul style="list-style-type: none"><li>• Validation: Random 20%</li></ul>  |
| <b>GMDH polynomial network</b>     | 20               | 20                | <ul style="list-style-type: none"><li>• Validation: Random 20%</li><li>• Layer connection: connect only to previous layer</li><li>• Overfitting protection control: Hold out sample percent: 20%</li></ul>  |
| <b>Cascade Correlation Network</b> | 3                | 6, 4, 1           | <ul style="list-style-type: none"><li>• Hidden layer kernel functions: Sigmoid &amp; Gaussian</li><li>• Model testing and validation: Random 20%</li></ul>  |

## *RBF Neural Network*

RBF Neural Network



RBF Neural Network





*Analysis of Variance*

| Method                                     | R <sup>2</sup><br>(%) | CV       | NMSE     | Correlation | RMSE      | MSE       | MAE       | MAPE      |
|--|-----------------------|----------|----------|-------------|-----------|-----------|-----------|-----------|
| <b>Multilayer<br/>Perceptron</b>           | 99.902                | 0.023519 | 0.000980 | 0.999567    | 42.326272 | 1791.5133 | 27.994853 | 12057.24  |
| <b>PNN/GRNN<br/>Neural Network</b>         | 99.958                | 0.015314 | 0.000416 | 0.999801    | 27.561308 | 759.6257  | 20.393533 | 4018.8622 |
| <b>RBD Network</b>                         | 99.851                | 0.029026 | 0.001493 | 0.999356    | 52.238191 | 2728.8286 | 30.969718 | 9530.1242 |
| <b>GMDH<br/>Polynomial<br/>Network</b>     | 99.989                | 0.007760 | 0.000107 | 0.999949    | 13.965366 | 195.03145 | 10.78587  | 6662.6184 |
| <b>Cascade<br/>Correlation<br/>Network</b> | 99.917                | 0.021708 | 0.000835 | 0.999657    | 39.067047 | 1526.2341 | 29.394567 | 4160.4599 |



*Data Normalization*

| R <sup>2</sup> (%) | CV       | NMSE     | Correlation | RMSE     | MSE      | MAE      | MAPE     | BEST METHOD                            |
|--------------------|----------|----------|-------------|----------|----------|----------|----------|--|
| 0.99913            | 3.030799 | 9.158879 | 0.999618    | 3.030804 | 9.185769 | 2.595512 | 3.000163 | <b>M4:</b> Multilayer Perceptron       |
| 0.99969            | 1.973454 | 3.88785  | 0.999852    | 1.973548 | 3.894889 | 1.890764 | 1        | <b>M2:</b> PNN/GRNN Neural Network     |
| 0.99862            | 3.740464 | 13.95327 | 0.999407    | 3.740555 | 13.99174 | 2.871323 | 2.371349 | <b>M5:</b> RBD Network                 |
| 1                  | 1        | 1        | 1           | 1        | 1        | 1        | 1.657837 | <b>M1:</b> GMDH Polynomial Network     |
| 0.99928            | 2.797423 | 7.803738 | 0.999708    | 2.797425 | 7.825581 | 2.725285 | 1.035233 | <b>M3:</b> Cascade Correlation Network |





*Variable Importance*

| Method                      | T1    | T2    | T3    | F1     | F2     | F3     | Most important variable |
|-----------------------------|-------|-------|-------|--------|--------|--------|-------------------------|
| Multilayer Perceptron       | 3.668 | 5.416 | 0.375 | 89.157 | 80.949 | 100.00 | F3                      |
| PNN/GRNN Neural Network     |       |       |       | 95.301 | 90.688 | 100.00 | F3                      |
| RBD Network                 | 0.347 | 0.192 | 0.108 | 0.078  | 25.139 | 100.00 | F3                      |
| GMDH polynomial network     |       |       |       |        | 100.00 |        | F2                      |
| Cascade Correlation Network | 5.103 | 1.906 | 0.187 | 5.086  | 6.006  | 100.00 | F3                      |



## *Heat Transfer Coefficient as function of Steam Mass Flow*

- In this case the only Input is the Steam mass flow at the main pipe
- The variable importance analysis leads us to such assumption
- The output is the heat transfer coefficient



*Analysis of Variance*

| Method                             | R <sup>2</sup><br>(%) | CV       | NMSE     | Correlation | RMSE      | MSE       | MAE       | MAPE      |
|------------------------------------|-----------------------|----------|----------|-------------|-----------|-----------|-----------|-----------|
| <b>Multilayer Perceptron</b>       | 99.975                | 0.011245 | 0.000253 | 0.999878    | 22.560377 | 508.97063 | 14.837764 | 13314.713 |
| <b>PNN/GRNN Neural Network</b>     | 99.925                | 0.019371 | 0.000750 | 0.999638    | 38.863604 | 1510.3797 | 26.997166 | 11408.283 |
| <b>RBD Network</b>                 | 99.730                | 0.036759 | 0.002702 | 0.998794    | 73.750907 | 5439.1963 | 44.793472 | 8957.221  |
| <b>GMDH polynomial network</b>     | 99.987                | 0.007992 | 0.000128 | 0.999938    | 16.033898 | 257.0859  | 11.020228 | 9985.6856 |
| <b>Cascade Correlation Network</b> | 99.988                | 0.007702 | 0.000119 | 0.999946    | 15.452697 | 238.78583 | 12.06805  | 6460.1994 |



NORTH CAROLINA AGRICULTURAL  
AND TECHNICAL STATE UNIVERSITY

---

## ***PART II: HEAT TRANSFER COEFFICIENT VS. PRESSURE DROP***

---

***PREDICTION OF PRESSURE DROP AND HEAT TRANSFER  
OF DEVELOPING AND FULLY DEVELOPED FLOW, USING  
MACHINE LEARNING TECHNIQUES***

AGGIES **DO**

# The purpose

- To establish the relationship between pressure drop and heat transfer in different flow regime.
- To use machine learning and experimental data to investigate in order to predict the heat transfer coefficient.

## Second Set of Experimental Data

- A smooth circular test section with an inner diameter of 11.5 mm, and maximum length-to-diameter ratio of 872.
- Measurement:
  - » Pressure drop and heat transfer measurements were taken at Reynolds numbers between 500 and 10,000 at different heat fluxes.
  - » Water was used as the test fluid and the Prandtl number ranged between 3 and 7.
  - » A total of 317 mass flow rate measurements, 34,553 temperature measurements and 2536 pressure drop measurements were taken.
  - » Pressure drop and heat transfer measurements were taken simultaneously.

# Development of Predictive Models

- Using machine learning techniques, the relationship between pressure drop and heat transfer was investigated.
- Correlations were developed to determine the relationship between heat transfer and pressure drop, as well as the average Nusselt numbers, in the laminar, transitional, quasi-turbulent and turbulent flow regimes, for both developing and fully developed flow in mixed convection conditions.



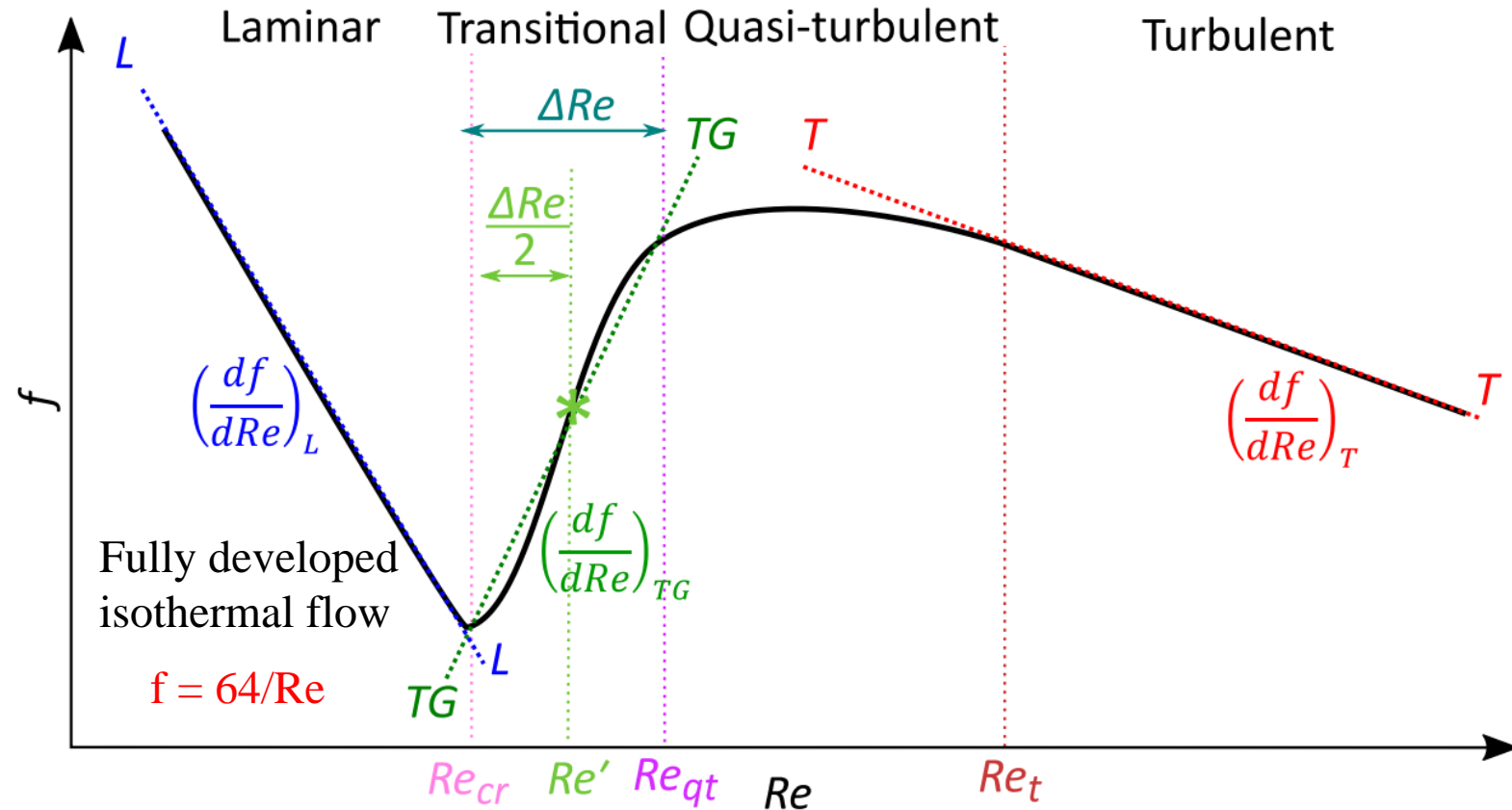
# Predictive Methods

1. Gene Expression Programming
2. Multilayer perceptron neural network (*MLP*)
3. Generalized regression neural network (GRNN)
4. Radial basis function network
5. Cascade Correlation Neural Network with Deterministic Weight
6. GMDH (Group Method of Data Handling) Polynomial Neural Network
7. LSTM (Long Short-Term Memory)

*The relationships between the friction factors and Reynolds Number [1]*

$$f = \frac{2\Delta PD}{L(x)\rho V^2} = \frac{\Delta P \rho D^5 \pi^2}{8\dot{m}^2 L(x)}$$

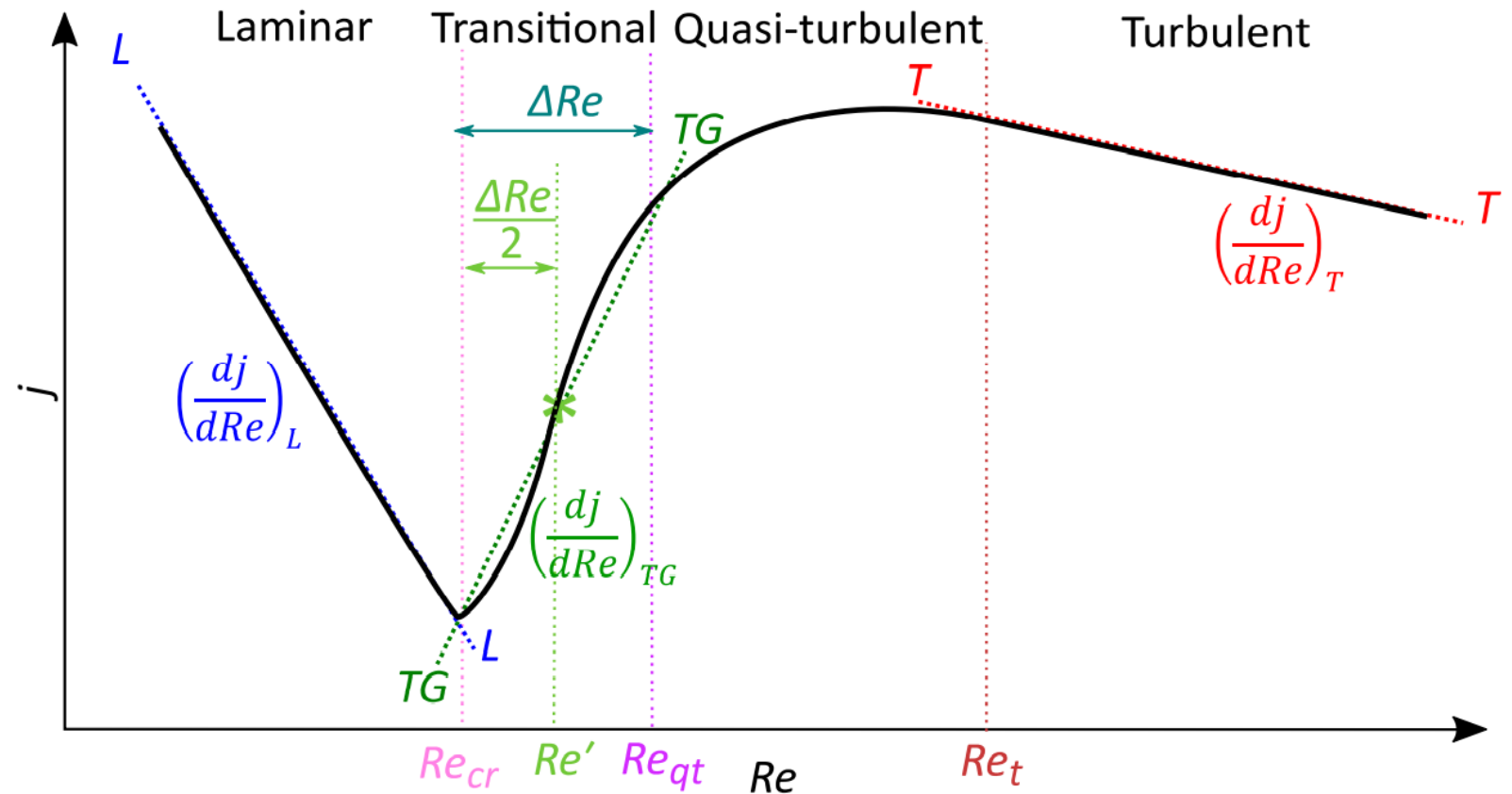
The friction factor ( $f$ ) is representing the loss of pressure of a fluid in a pipe due to the interactions in between the fluid and the pipe.



[1] M. Everts, J.P. Meyer, Heat transfer of developing and fully developed flow in smooth horizontal tubes in the transitional flow regime, Int. J. Heat Mass Transf. 117 (2018) 1331–1351.

*The relationships between the Colburn j-factors and Reynolds Number [3]*

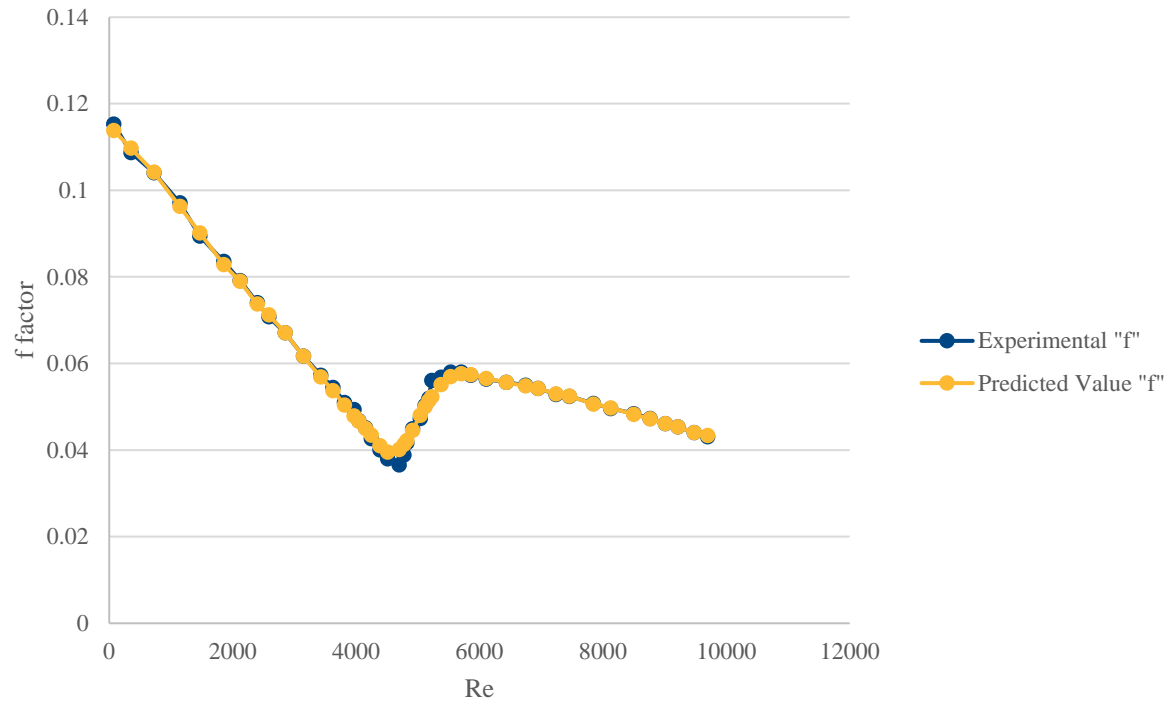
**J Factor** is A dimensionless factor  
for heat transfer coefficient for  
calculating the heat  
transfer coefficient



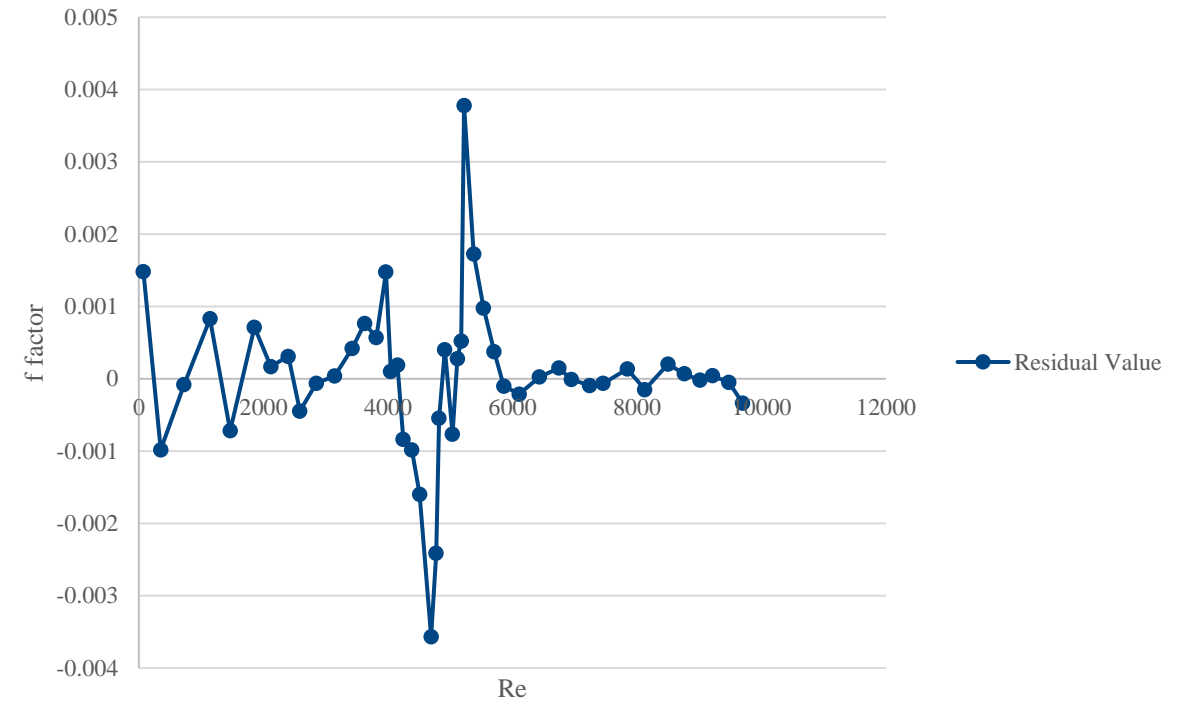
## *General Regression Neural Network (GRNN): 3 kW/m<sup>2</sup>*

$$0 \text{ m} \leq L \leq 2 \text{ m},$$

General Regression Neural Network (GRNN): 3 kW/m<sup>2</sup>



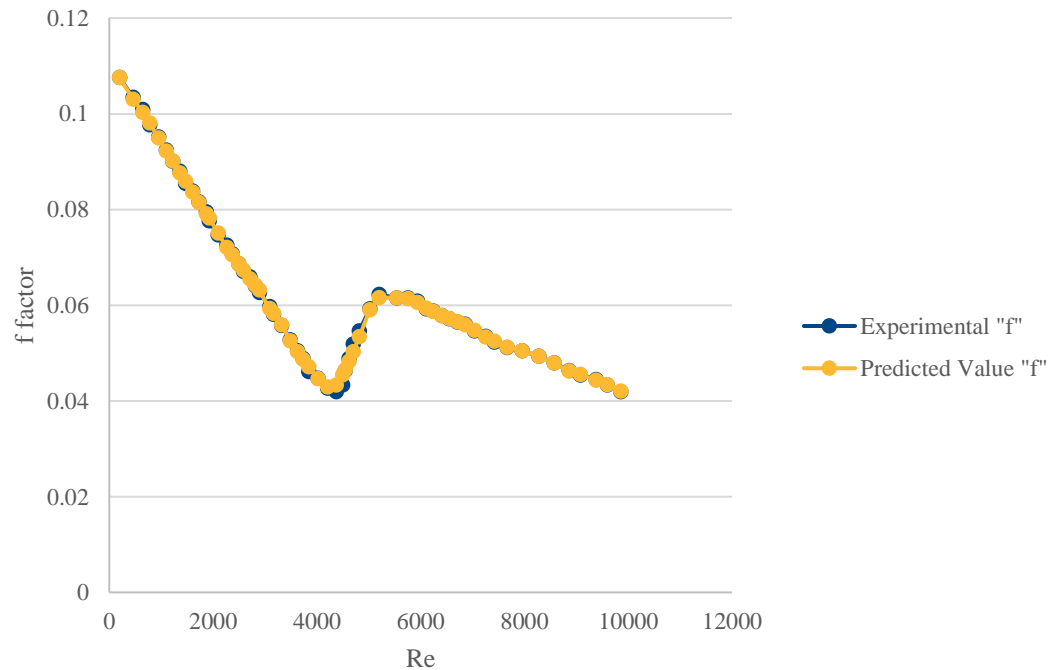
General Regression Neural Network (GRNN): 3 kW/m<sup>2</sup>



## *General Regression Neural Network (GRNN): 0 kW/m<sup>2</sup>*

$$0 \text{ m} \leq L \leq 2 \text{ m},$$

General Regression Neural Network (GRNN): 0 kW/m<sup>2</sup>



General Regression Neural Network (GRNN): 0 kW/m<sup>2</sup>

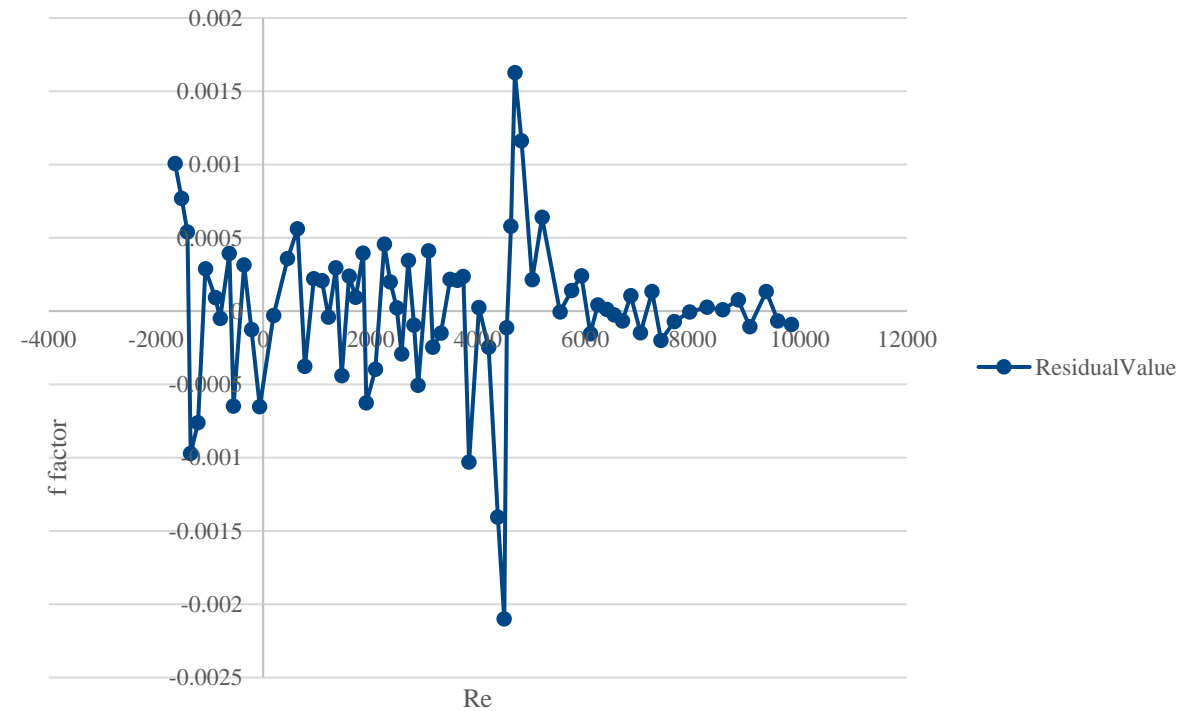
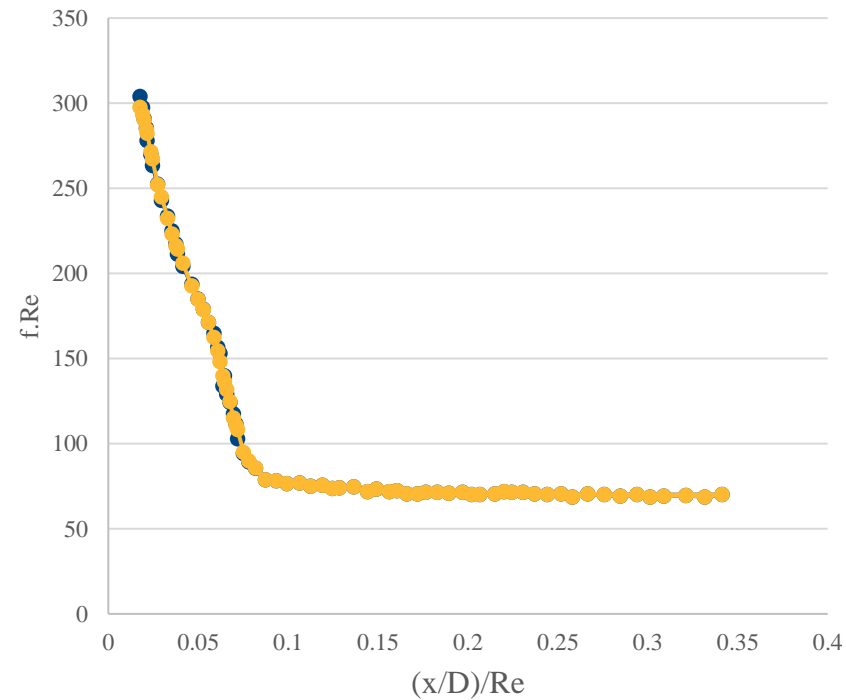


*Fig 6: Comparison of the product of the friction factor and Reynolds number ( $f \cdot Re$ ) as a function of dimensionless axial distance*

General Regression Neural Network (GRNN): 0 kW/m<sup>2</sup>



General Regression Neural Network (GRNN): 0 kW/m<sup>2</sup>

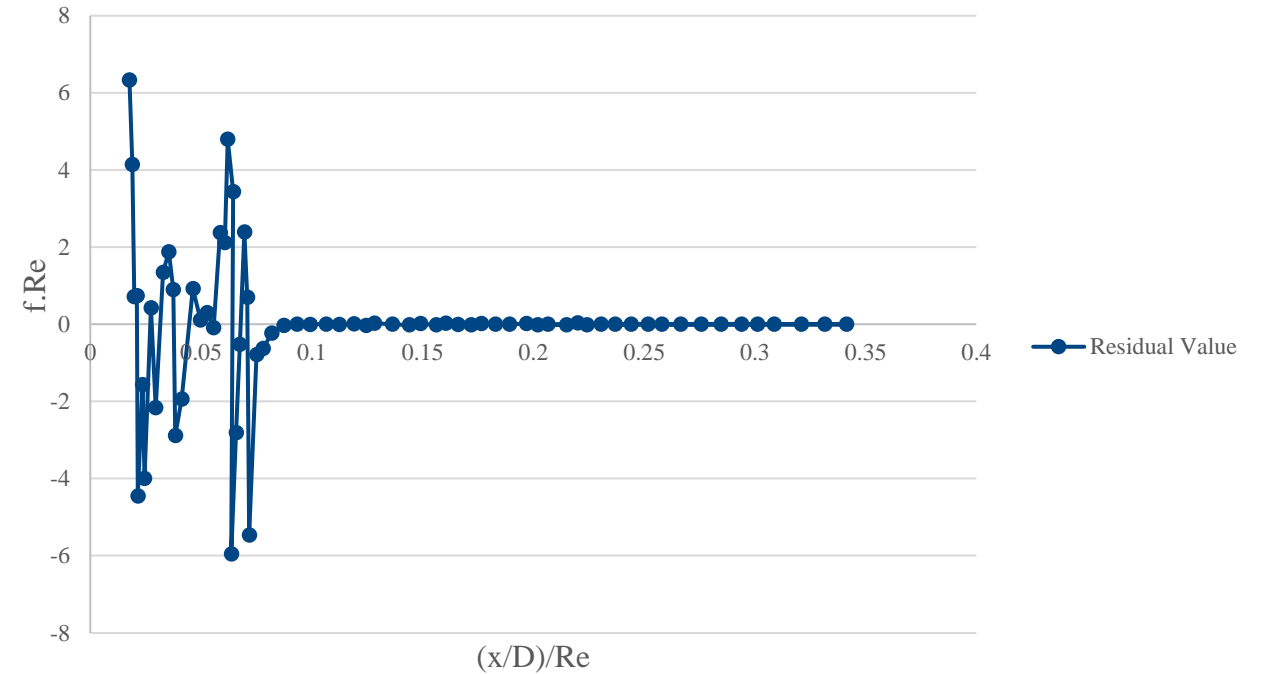


*Fig 6: Comparison of the product of the friction factor and Reynolds number ( $f \cdot Re$ ) as a function of dimensionless axial distance*

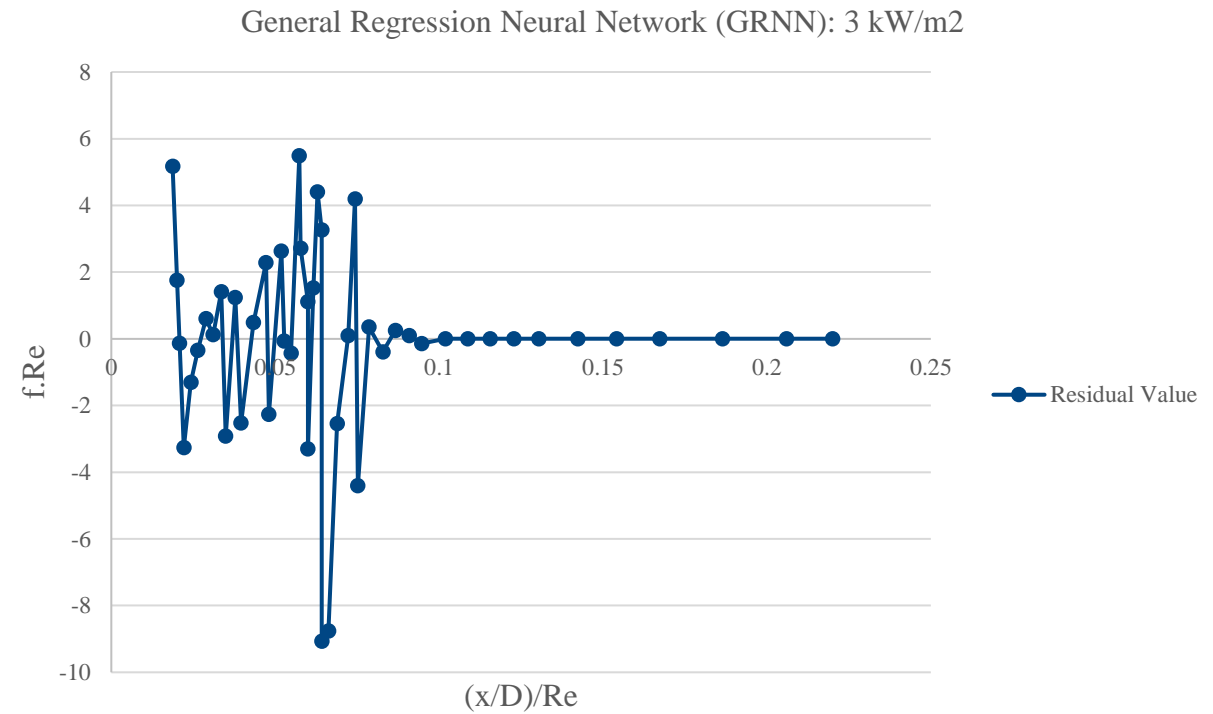
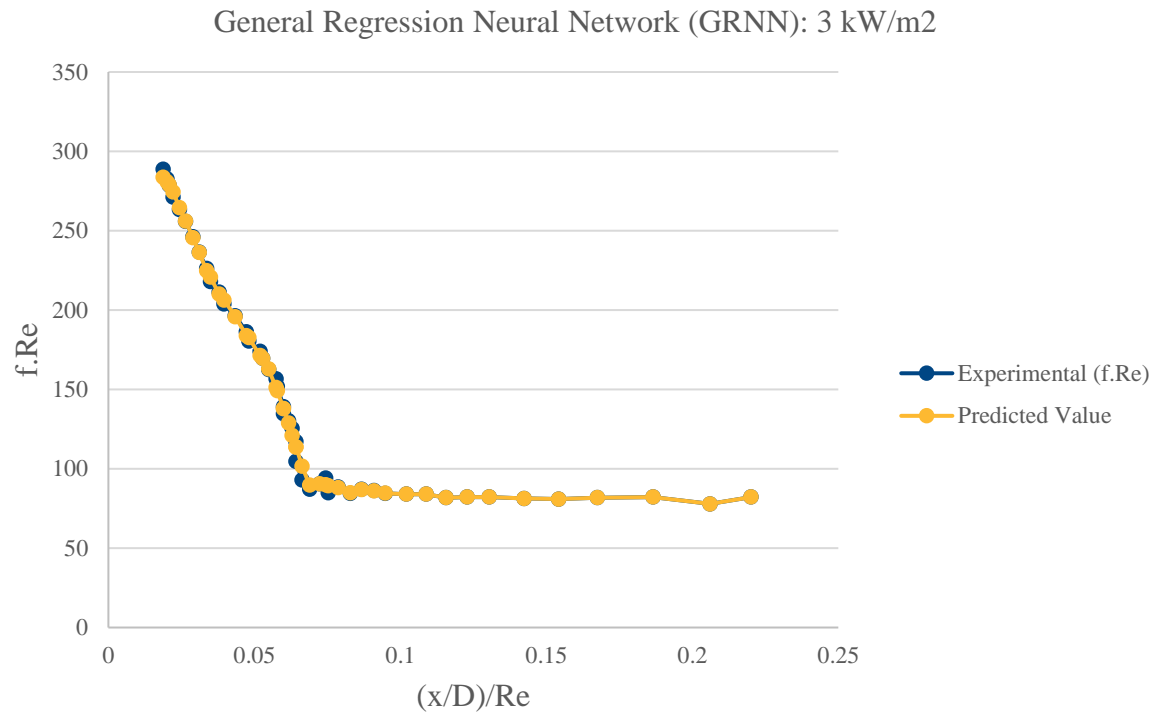
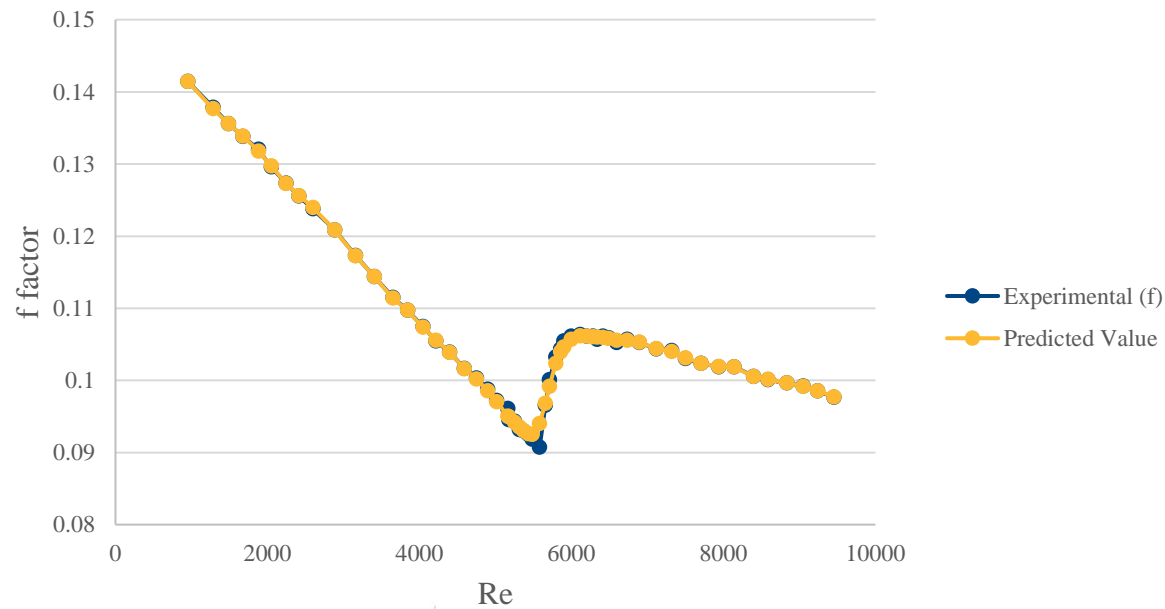


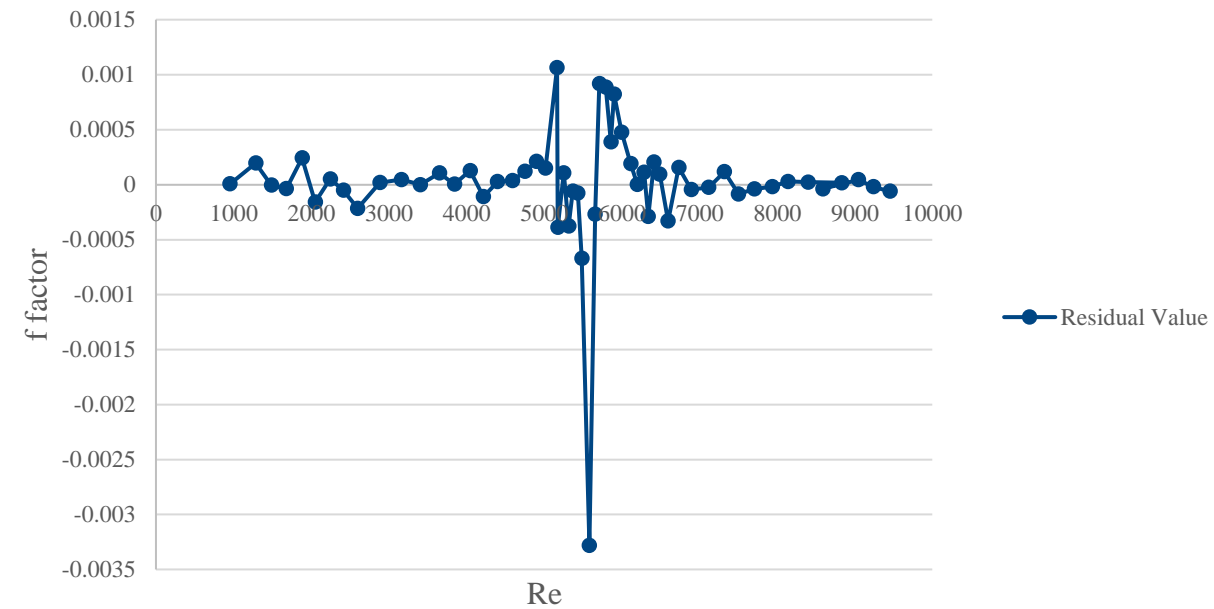


*Fig. 8. Comparison of the pressure drop and heat transfer results in terms of the friction factors for  $0\text{ m} < L < 8\text{ m}$  as a function of Reynolds number, at heat fluxes of  $1\text{ kW/m}^2$*

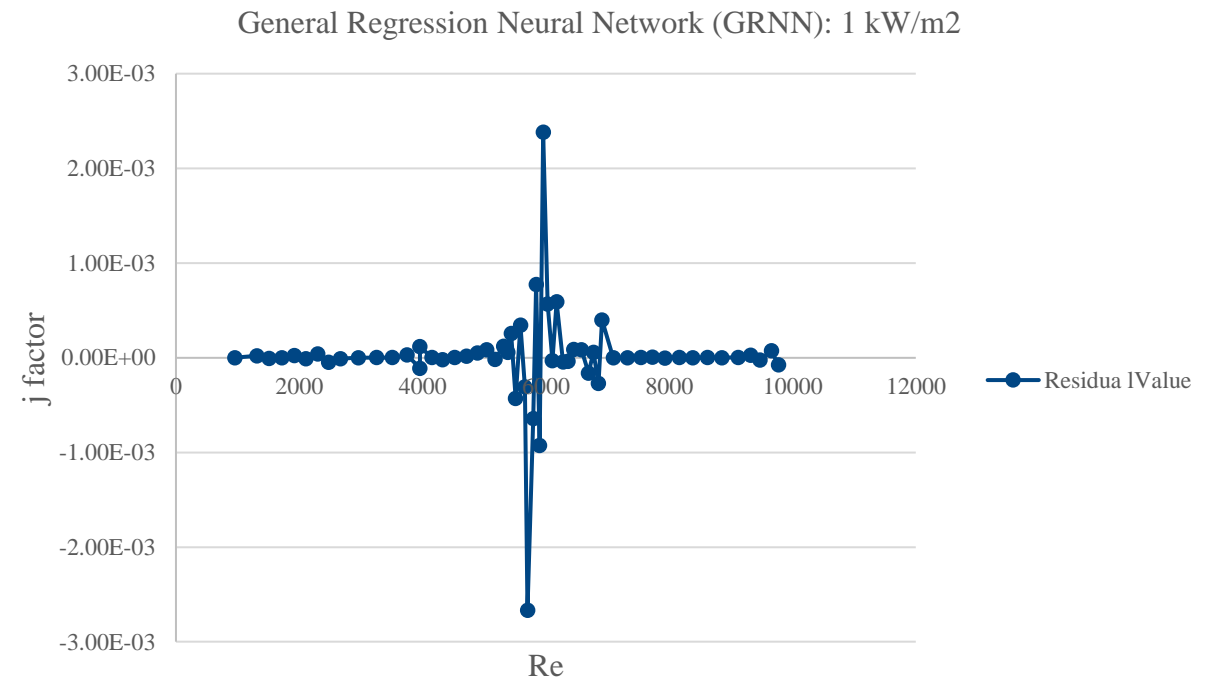
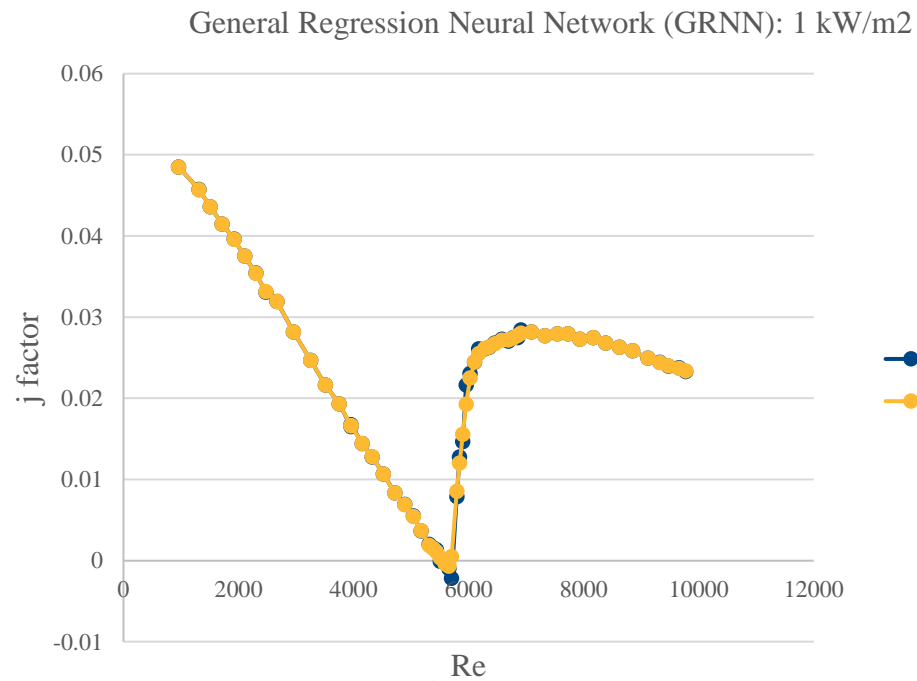
General Regression Neural Network (GRNN):  $1\text{ kW/m}^2$



General Regression Neural Network (GRNN):  $1\text{ kW/m}^2$

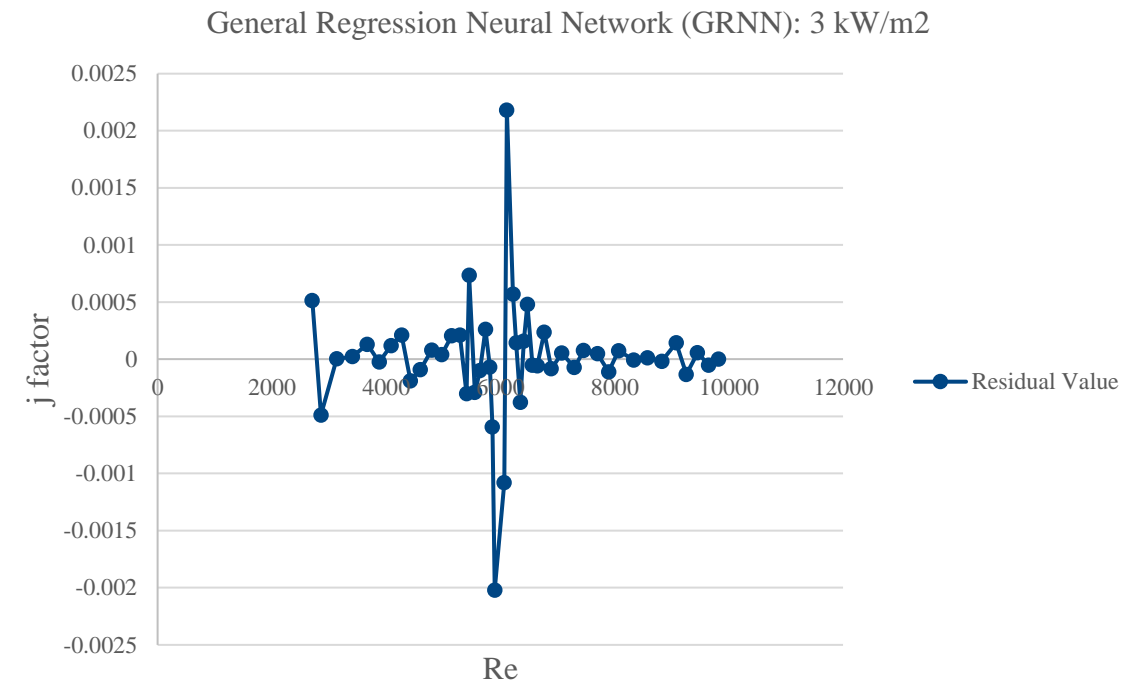
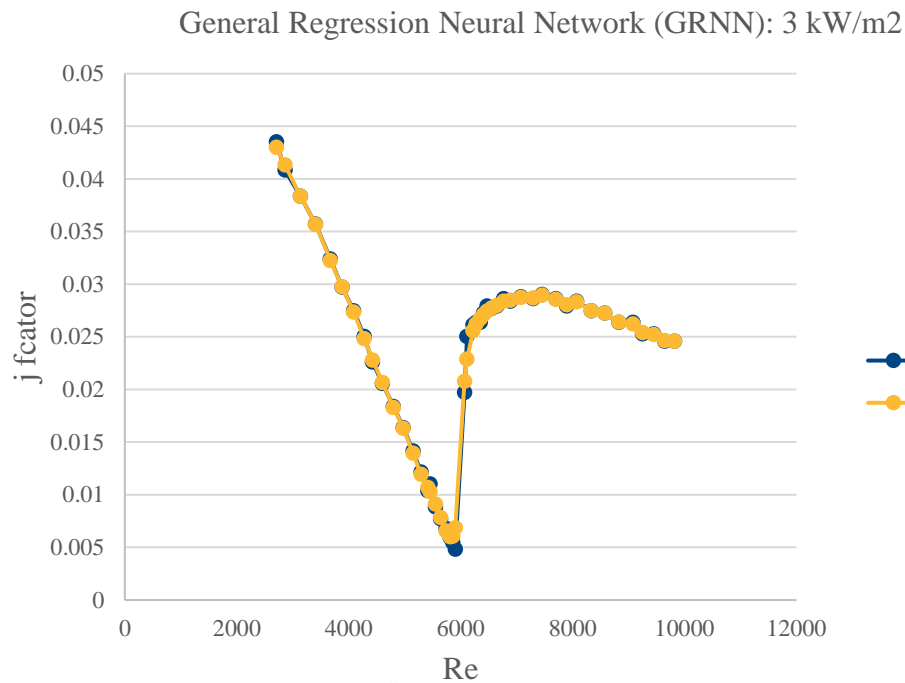


*Comparison of the pressure drop and heat transfer results in terms of the average **Colburn j-factors** for  $0\text{ m} < L < 8\text{ m}$  as a function of Reynolds number, at heat fluxes of  $1\text{ kW/m}^2$*





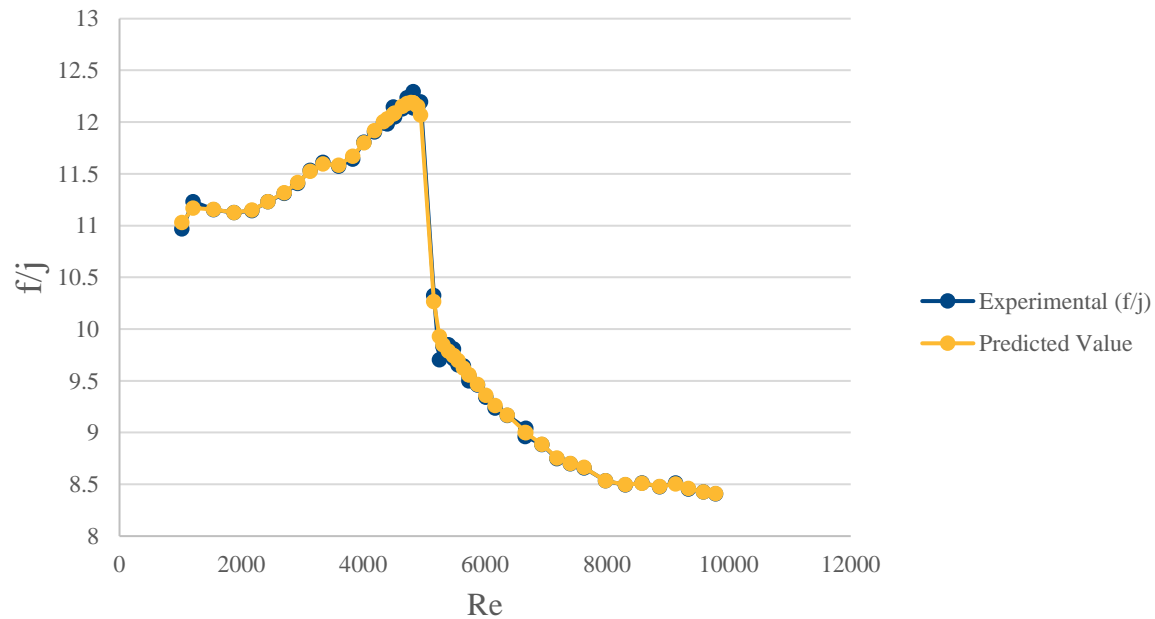
*Comparison of the pressure drop and heat transfer results in terms of the average Colburn  $j$ -factors for  $0\text{ m} < L < 8\text{ m}$  as a function of Reynolds number, at heat fluxes of  $3\text{ kW/m}^2$*



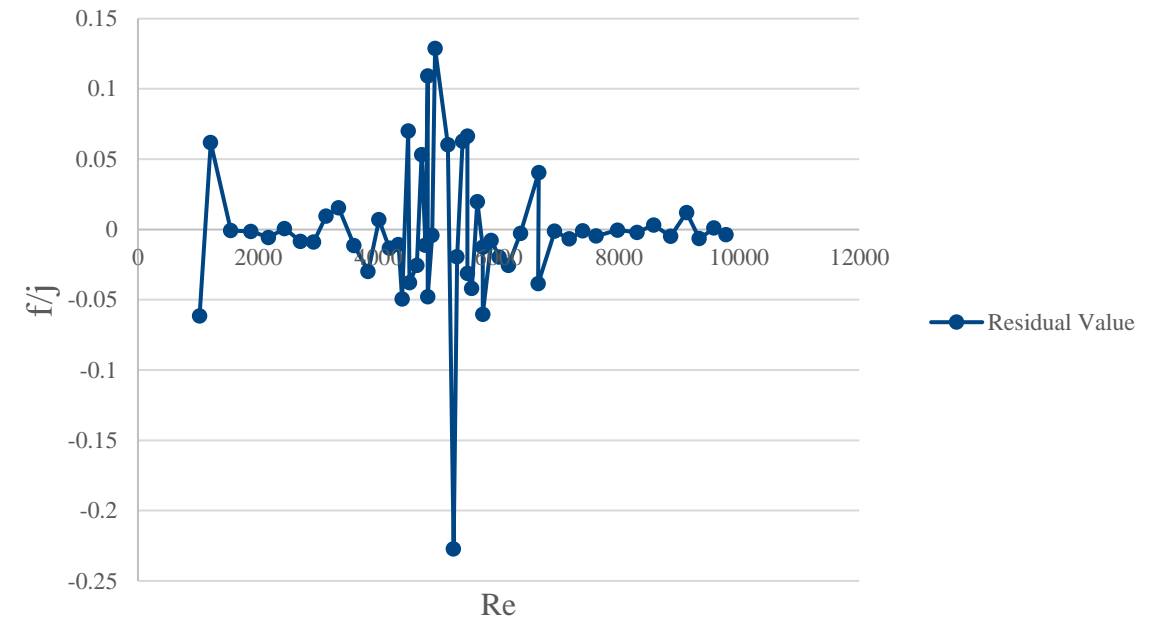


*Comparison of the friction factors divided by the average Colburn  $j$ -factors as a function of Reynolds number for  $0\text{ m} < L < 8\text{ m}$  at a heat flux of  $3\text{ kW/m}^2$*

General Regression Neural Network (GRNN):  $3\text{ kW/m}^2$



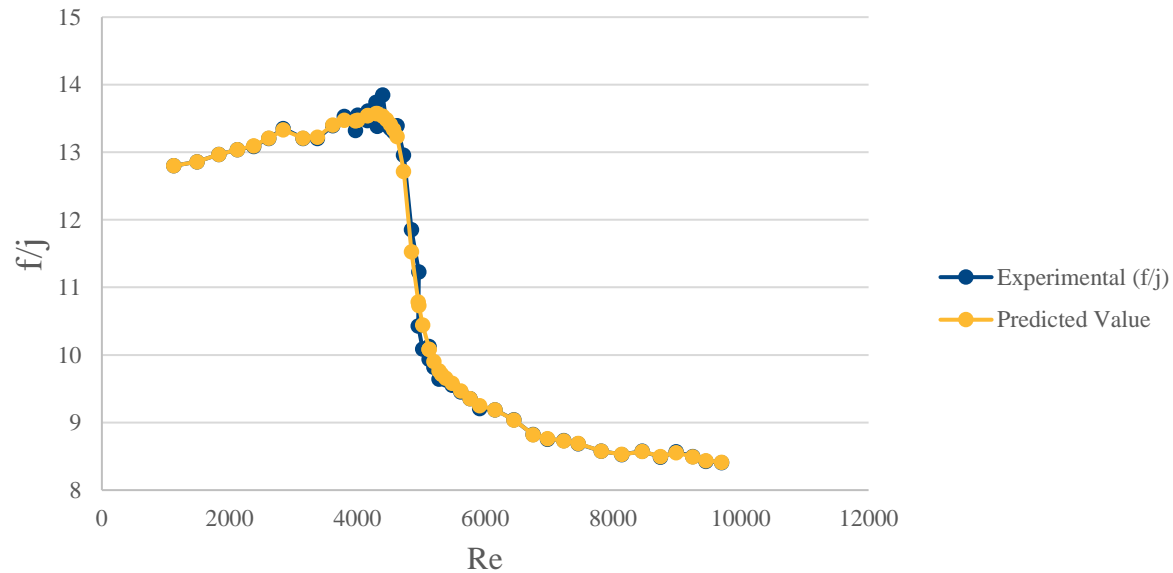
General Regression Neural Network (GRNN):  $3\text{ kW/m}^2$



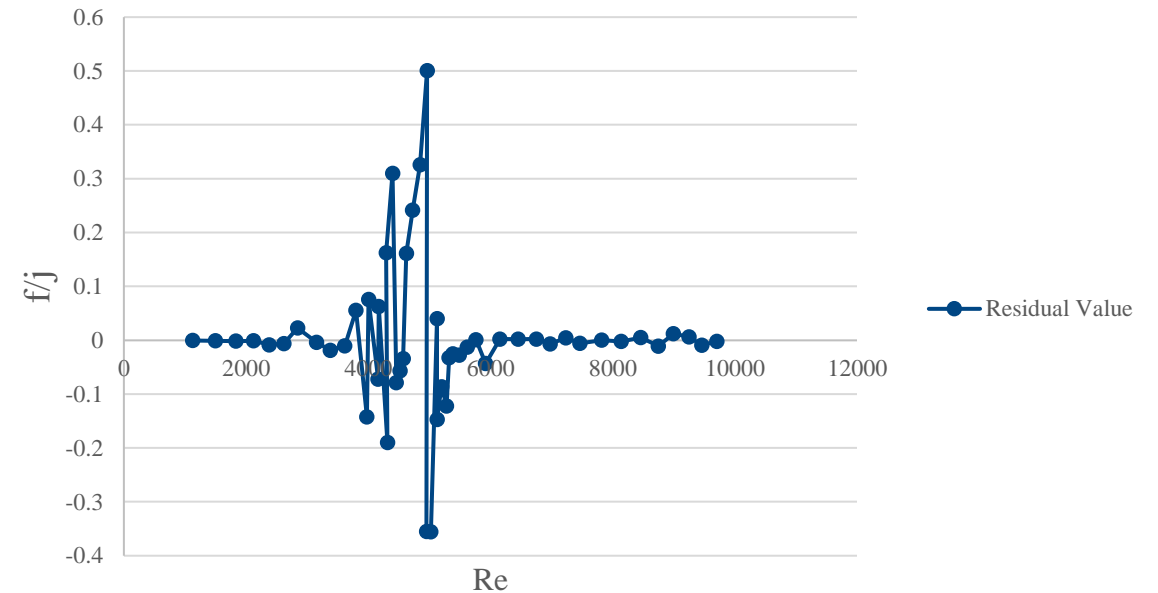


*Comparison of the friction factors divided by the average Colburn j-factors as a function of Reynolds number for  $0\text{ m} < L < 2\text{ m}$  at a heat flux of  $3\text{ kW/m}^2$*

General Regression Neural Network (GRNN):  $3\text{ kW/m}^2$



General Regression Neural Network (GRNN):  $3\text{ kW/m}^2$





### *Analysis of Variance*

|  | <u>Figure 5: 0</u><br><u>kW/m2</u> | <u>Fig 5: 3</u><br><u>kW/m2</u> | Fig6a_B0.csv | Fig6a_Y3.csv | Fig8_f_1.csv |
|--|------------------------------------|---------------------------------|--------------|--------------|--------------|
| <b>Proportion of variance explained by model (R<sup>2</sup>)</b><br><b>%</b> | 99.968%                            | 99.682                          | 99.935       | 99.838       | 99.815       |
| <b>Coefficient of variation (CV)</b>   | 0.007094                           | 0.018168                        | 0.015090     | 0.018976     | 0.004997     |
| <b>Normalized mean square error (NMSE)</b>                                   | 0.000323                           | 0.003183                        | 0.000645     | 0.001616     | 0.001855     |
| <b>Correlation between actual and predicted</b>                              | 0.999840                           | 0.998468                        | 0.999679     | 0.999201     | 0.999083     |
| <b>Maximum error</b>   | 0.0021012                          | 0.0037786                       | 6.3281898    | 9.0706368    | 0.0032808    |
| <b>RMSE (Root Mean Squared Error)</b>  | 0.0005277                          | 0.0010562                       | 1.8890273    | 2.7823118    | 0.0005358    |
| <b>MSE (Mean Squared Error)</b>  | 0.0000003                          | 0.0000011                       | 3.568424     | 7.7412589    | 0.0000003    |
| <b>MAE (Mean Absolute Error)</b>   | 0.0003513                          | 0.0006473                       | 0.9776852    | 1.7255757    | 0.0002439    |
| <b>MAPE (Mean Absolute Percentage Error)</b>                                 | 0.5314583                          | 1.2717376                       | 0.5700633    | 1.3014959    | 0.2448627    |



### *METHODOLOGY Developed*

#### **Laminar:**

$$48 \leq Re \leq 3217, 2.9 \leq Pr \leq 282, 5.5 \leq Gr \leq 4.5 \times 10^4, 41 \leq Gr^* \leq 7.3 \times 10^6$$

#### **Transitional:**

$$2520 \leq Re \leq 3361, 5.4 \leq Pr \leq 6.8, 2.8 \times 10^4 \leq Gr \leq 3.2 \times 10^4, \\ 6.1 \times 10^4 \leq Gr^* \leq 3.7 \times 10^5$$

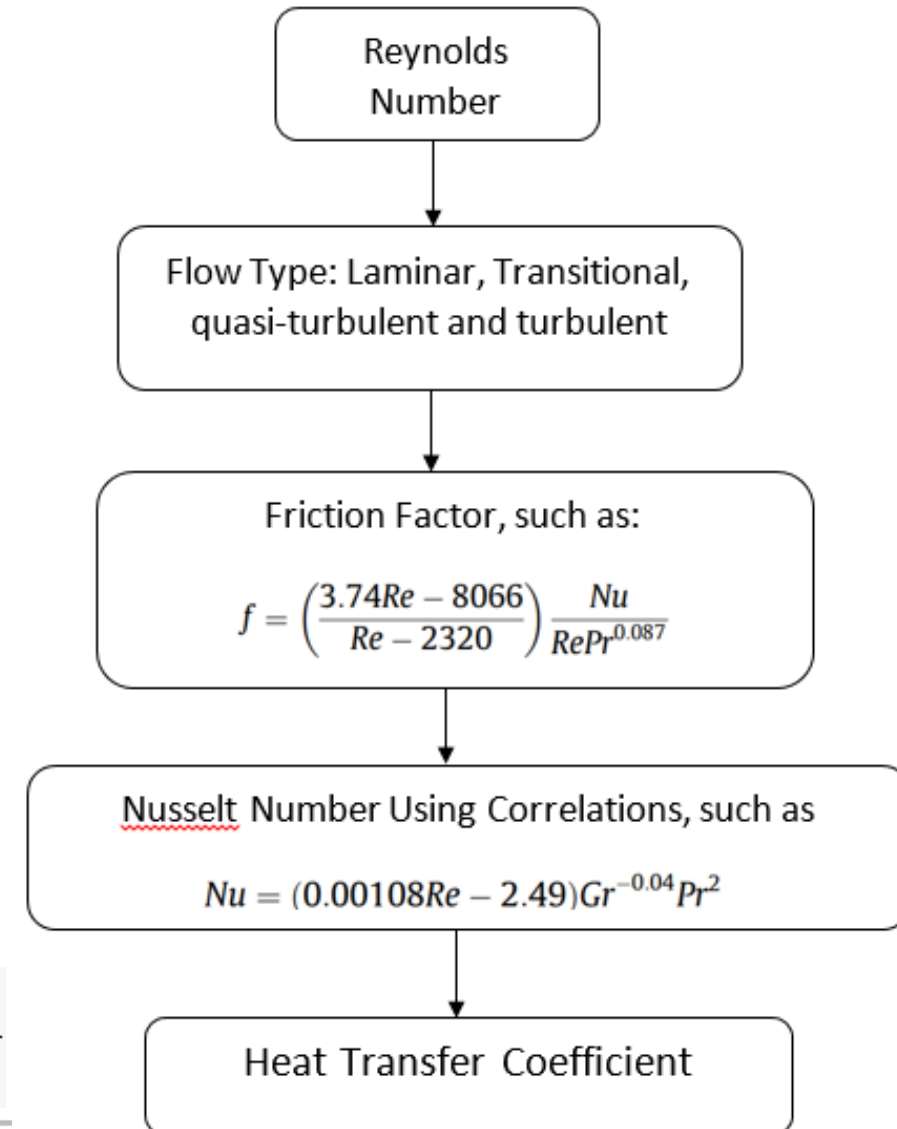
#### **Quasi-turbulent and turbulent:**

$$2804 \leq Re \leq 9787, 5.5 \leq Pr \leq 6.9, 8.9 \times 10^2 \leq Gr \leq 1.4 \times 10^4, \\ 5.9 \times 10^4 \leq Gr^* \leq 3.6 \times 10^5$$

The average Colburn j-factors of the different tube lengths as a function of Reynolds number at different heat fluxes

$$Nu = \frac{h L}{\lambda}$$

AGGIES DO







---

## *Conclusions and Future Work*

---

## *Conclusions*

- ❖ The heat transfer coefficient depends mainly on the mass flow of steam. Temperature and pressure are secondary.
- ❖ Machine learning techniques: GMDH polynomial network and PNN/GRNN neural network are the best in predicting heat transfer coefficient.
- ❖ For both sets of experimental data, a methodology is developed to predict the heat transfer coefficient
- ❖ Our next goal is to predict the heat transfer coefficient using dynamic CFD modeling of an Inconel 740H alloy boiler outlet header.

# Part III: Steam Header Design Progress



UNC CHARLOTTE

---

*The* WILLIAM STATES LEE COLLEGE *of* ENGINEERING

April 2022  
Michael Zimnoch



UNC CHARLOTTE

---

*The* WILLIAM STATES LEE COLLEGE *of* ENGINEERING

# Designing Headers

- Header is designed using three materials: P22, P91, IN740.
  - Each header will be designed in accordance with a series of ASME BPVC Codes
    - Section I: General Design Requirements
    - Section II: Material Properties
    - Section III-NH: Evaluation of Components in Elevated Temperature Service
    - Section VIII-2: Alternative Rules – Design Fatigue Curves
  - IN740 material properties will be taken from Special Metals
  - The life expectancy of each header will be evaluated using
    - ASME BPVC Section VIII-2
    - STP-PT-070
    - ASME FFS-1/ API 579-1



<https://www.indiamart.com/proddetail/boiler-headers-4962339955.html>



UNC CHARLOTTE

*The WILLIAM STATES LEE COLLEGE of ENGINEERING*

# Geometry Design

- The wall thickness of the header and tubes were found using the processes outlined in subsection PG-27.2.1

Tube thickness

$$t = \frac{Pd_o}{2S + P} + 0.005d_o$$

$$d_o = \text{OD Tube} = 2.0''$$

$P$  = Maximum allowable working pressure (2450 psi)

$S$  = Maximum Allowable Stress at Design Temperature

$$S_{P22} = 53.57 \text{ MPa at } 541^\circ\text{C}$$

$$S_{P91} = 108.4 \text{ MPa at } 541^\circ\text{C}$$

$$S_{IN740} = 276 \text{ MPa at } 541^\circ\text{C}$$

$$t_{P22} = 0.282''$$

$$t_{P91} = 0.155''$$

$$t_{IN740} = 0.070''$$



UNC CHARLOTTE

The WILLIAM STATES LEE COLLEGE of ENGINEERING

# Geometry Design - Header

$$\text{Header thickness} \longleftarrow t = \frac{PD}{2SE + 2yP} + C$$

**D** = Outer Diameter

P22 - 22.25"

P91 - 19.07"

IN740 - 16.87"

**ID** = 15.25 for all models

**P** = Maximum allowable  
working pressure = 2450 psi

**C** = Minimum allowance for  
threading stability = 0

**f** = 0, tubes will be welded in.

**E** = Efficiency = 0.797

$$E = \frac{p - d}{p}$$

**p** = Pitch = 6"

**d** = Diameter of opening = 1.219"

**S** = Maximum Allowable Stress at  
Design Temperature

**t** = Wall Thickness

P22 - 3.45"

P91 - 1.91"

IN740 - 0.81"

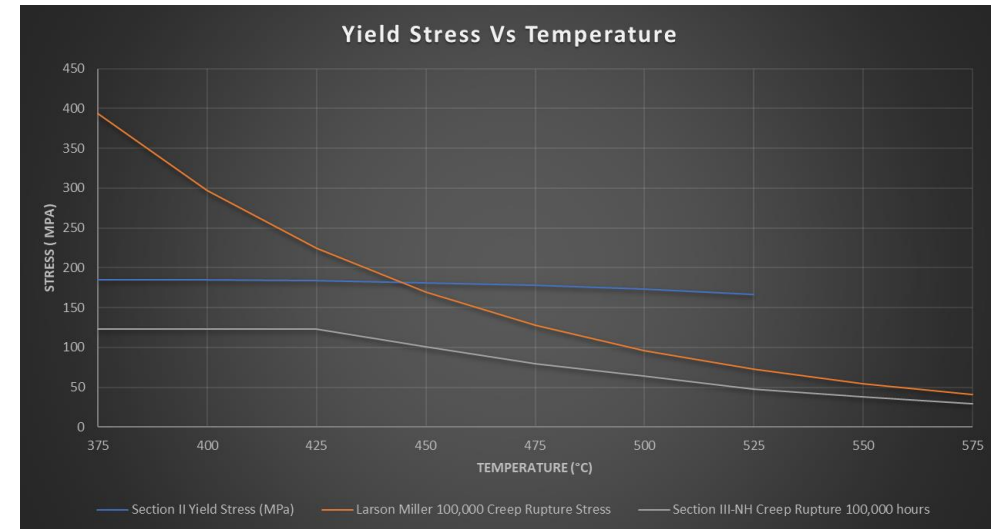
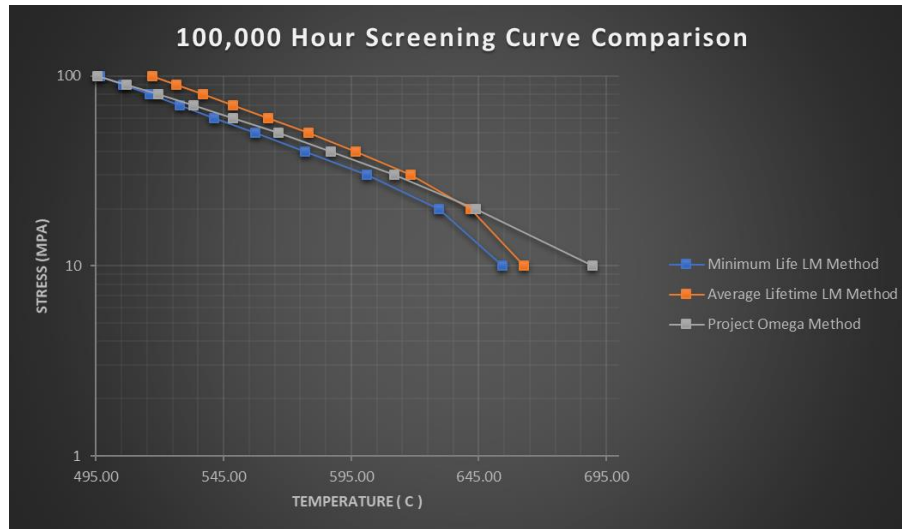


UNC CHARLOTTE

The WILLIAM STATES LEE COLLEGE of ENGINEERING

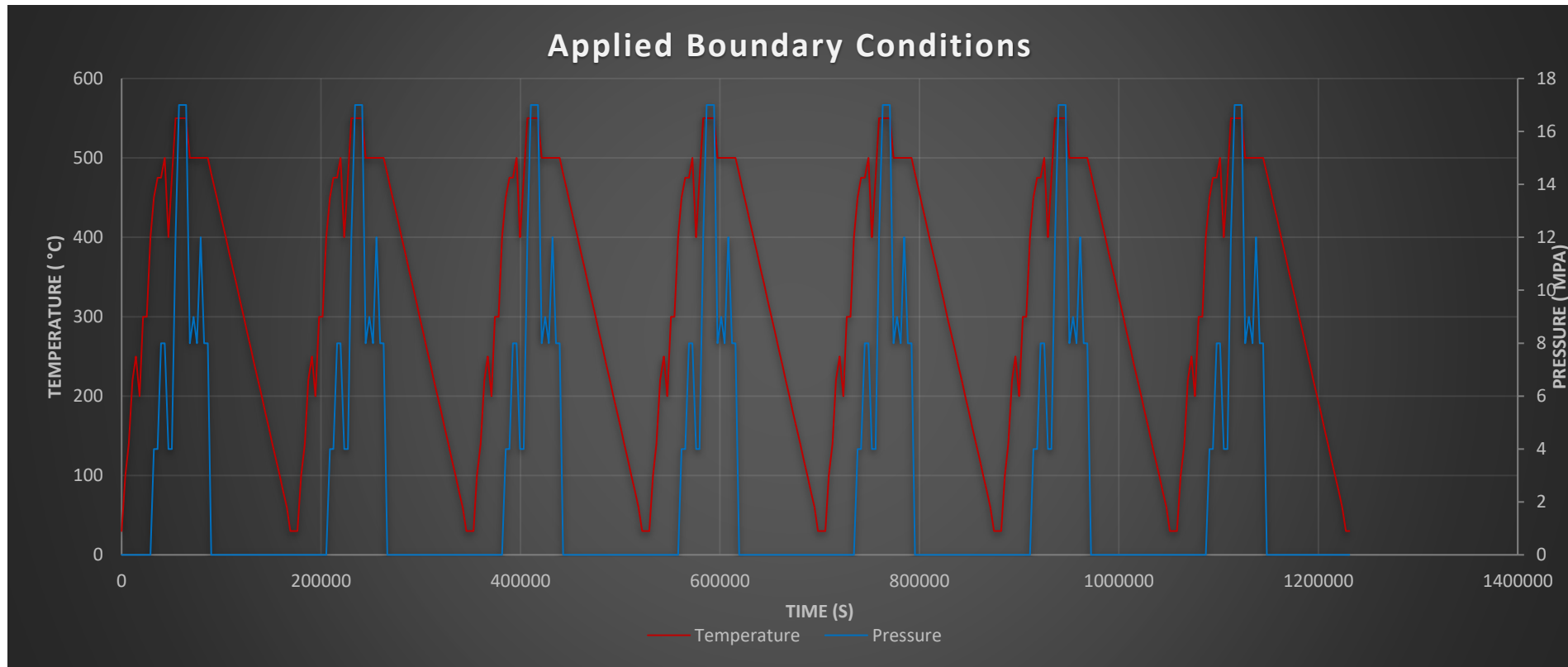
# Creep Rupture

- API 579-1/ASME FFS-1 provides 3 options to determine the creep rupture at a given time.
  - Project Omega Method
  - Larson Miller Method – Average Lifetime
  - Larson Miller Method – Minimum Lifetime
- The Larson Miller Minimum Lifetime method was chosen to reflect the most conservative case.
- The lower value of the yield stress of the material or the stress to cause creep rupture at 100,000 hours was used to evaluate the model for shakedown.



# Shakedown

- Idealized pressure and temperature profiles were generated from data provided by the power plant.
- The idealized cycle was ran 7 times to evaluate the model for shakedown.
- Peak Temperature: 550 °C
- Peak Pressure: 17 MPa





# Geometry Design - Header

$$\text{Header thickness} \longleftarrow t = \frac{PD}{2SE + 2yP} + C$$

**D** = Outer Diameter

P22 - 22.25"

P91 - 19.07"

IN740 - 16.87"

**ID** = 15.25 for all models

**P** = Maximum allowable  
working pressure = 2450 psi

**C** = Minimum allowance for  
threading stability = 0

**f** = 0, tubes will be welded in.

**E** = Efficiency = 0.797

$$E = \frac{p - d}{p}$$

**p** = Pitch = 6"

**d** = Diameter of opening = 1.219"

**S** = Maximum Allowable Stress at  
Design Temperature

**t** = Wall Thickness

P22 - 3.45"

P91 - 1.91"

IN740 - 0.81"

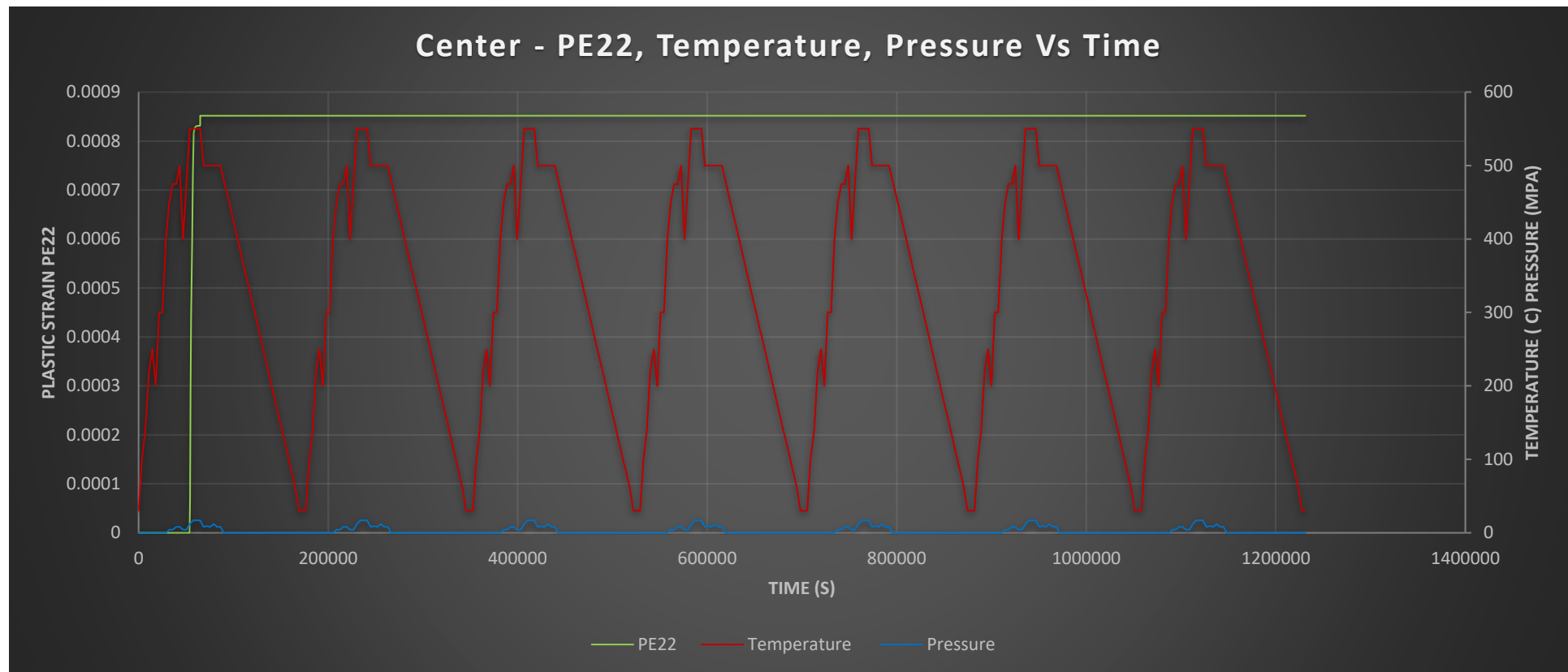


UNC CHARLOTTE

The WILLIAM STATES LEE COLLEGE of ENGINEERING

# Shakedown

- The P22 model was found to shakedown during the first cycle.



# Material Model Verification

- Steps were also taken to validate the application of the material model in Abaqus.
- A paper evaluating a P91 header was recreated [1].
- The material used was a P91 Two-Layer Visco-Plastic model.

- $\varepsilon_p^{el} = \frac{1+v}{K_p} \boldsymbol{\sigma}_p - \frac{v}{K_p} tr(\boldsymbol{\sigma}_p) \mathbf{I}$
- $\varepsilon_v^{el} = \frac{1+v}{K_v} \boldsymbol{\sigma}_v - \frac{v}{K_v} tr(\boldsymbol{\sigma}_v) \mathbf{I}$
- $\boldsymbol{\sigma}_v = \mathbf{K}_v : (\boldsymbol{\varepsilon} - \boldsymbol{\varepsilon}_v)$
- $\boldsymbol{\sigma}_p = \mathbf{K}_p : (\boldsymbol{\varepsilon} - \boldsymbol{\varepsilon}_p)$
- $\boldsymbol{\sigma} = \boldsymbol{\sigma}_p + \boldsymbol{\sigma}_v$

- $\sigma^0 = k + Q_\infty(1 - \exp(-bp))$
- $\dot{\alpha}_i = C_i \dot{p} \frac{1}{\sigma^0} (\boldsymbol{\sigma}_p - \boldsymbol{\alpha}_i) - \gamma_i \boldsymbol{\alpha}_i \dot{p} + \frac{1}{C_i} \boldsymbol{\alpha}_i \dot{C}_i$
- $\frac{\Delta \sigma}{2} - k = \frac{C_i}{\gamma_i} \tanh(\gamma_i \frac{\Delta \varepsilon_p}{2})$
- $\dot{\varepsilon}_v = \frac{3}{2} A [f(\boldsymbol{\sigma}_v)]^n \frac{S_v}{f(\boldsymbol{\sigma}_v)}$
- $B = \frac{K_v}{K_v + K_p}$



# Material Model Verification

- The temperature and pressure profiles were provided by [1].
  - Maximum Operating Pressure: 17 MPa
  - Maximum Operating Temperature: 490 °C

The failure criteria was taken as the largest Ostergren parameter  $\Delta\varepsilon_{in}\sigma_{max}$  shown in the following equation [1]:

$$N_F = C(\Delta\varepsilon_{in}\sigma_{max})^\beta$$

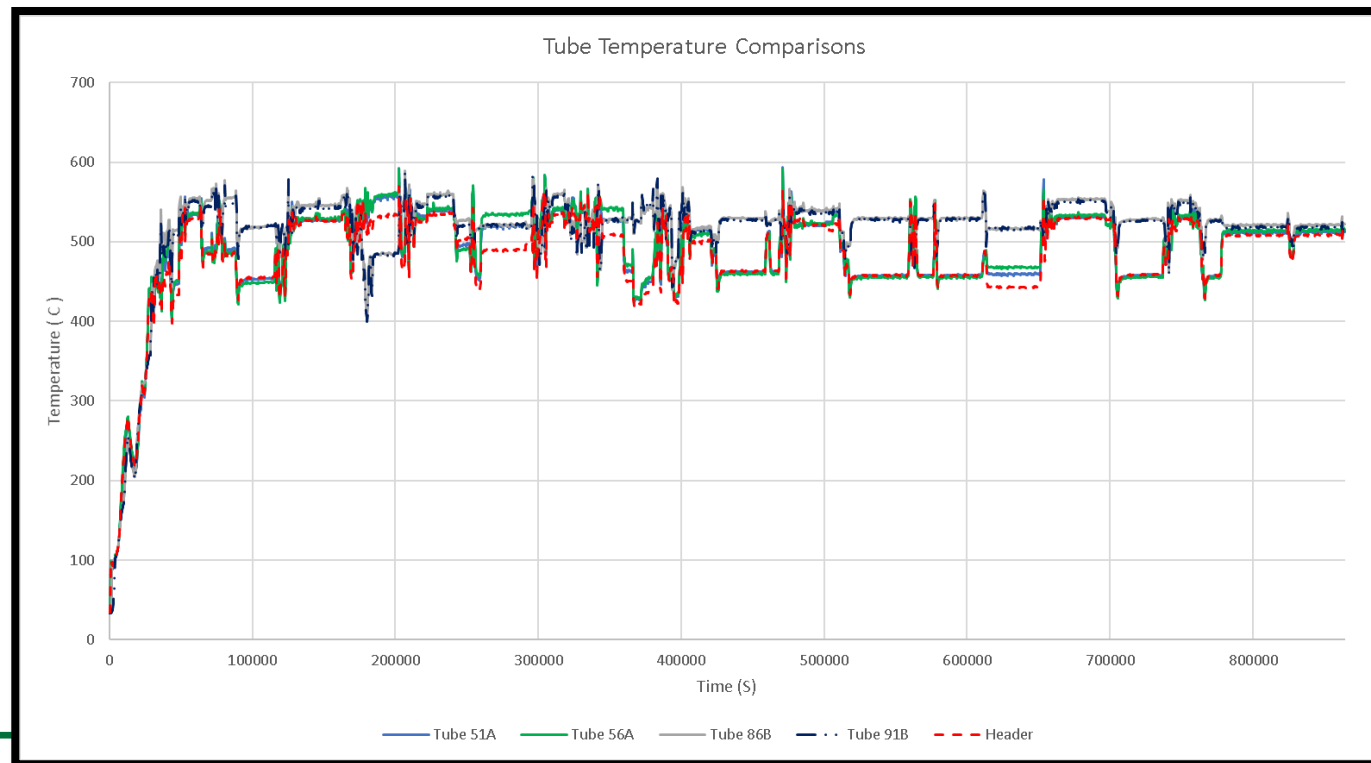
- C &  $\beta$  are material constants determined from [1] and taken as 4,500 and -1.6 respectively.

| Model          | Location | Cycles To Failure | Years To Failure |
|----------------|----------|-------------------|------------------|
| T.P. Farragher | Center   | 2,178             | 41.9             |
| T.P. Farragher | Edge     | 1,954             | 37.6             |
| M. Zimnoch     | Center   | 2,211             | 42.5             |
| M. Zimnoch     | Edge     | 2,042             | 39.3             |



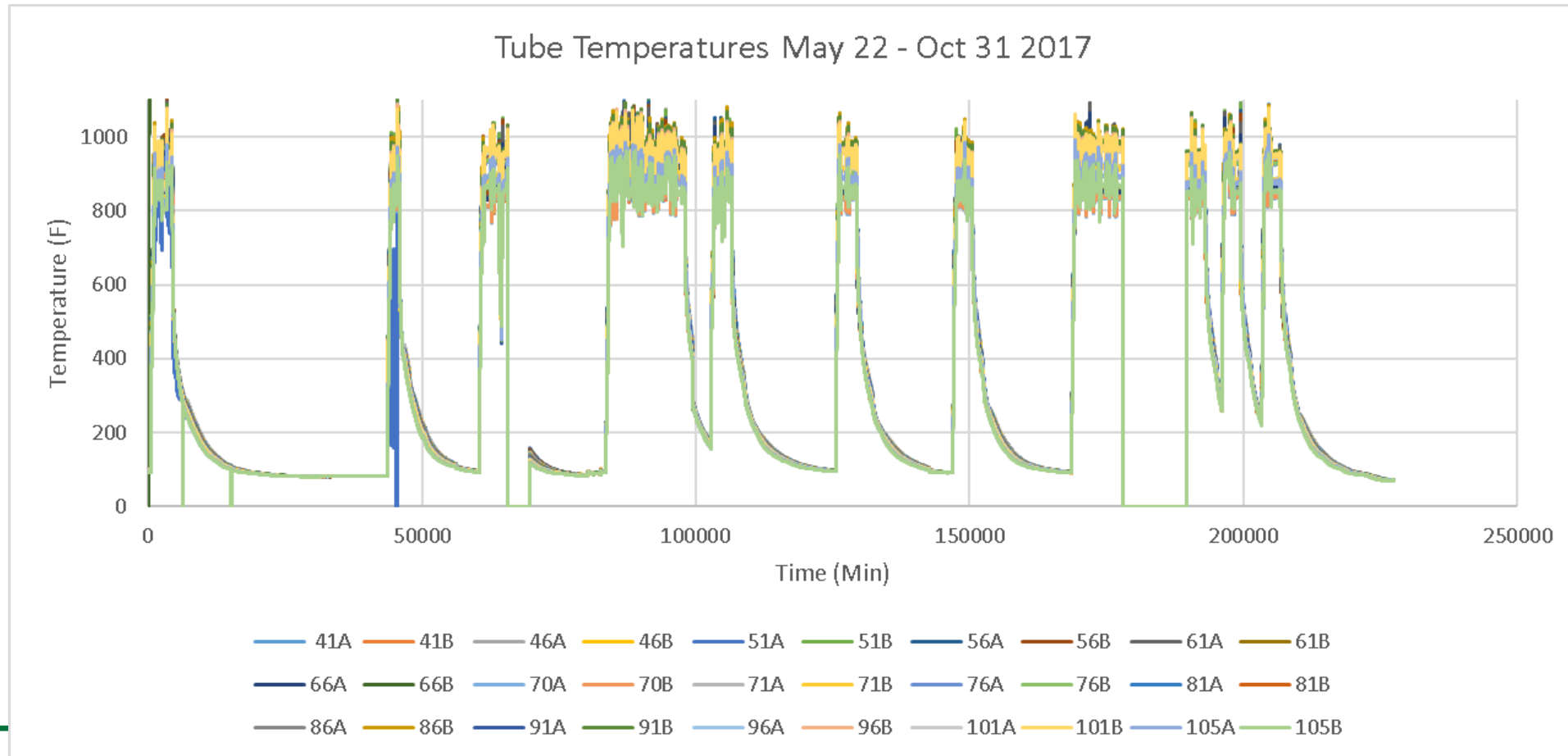
# Material Model Verification

- The methodology was applied to the headers under normal loading scenarios and found an unrealistic lifespan on the order of >300 years for all materials.
- Additional thermal data shows that the tube temperatures can significantly exceed the design temperature of the header.
- Some tubes have an average temperature 30 °C higher than the average header temperature.



# Material Model Verification

- Additional thermal data shows that the tube temperatures can significantly exceed the design temperature of the header 1005 °F (540.6 °C) routinely throughout the year.



# Material Model Verification

- The maximum tube temperatures exceed the design temperature of the header of 1005 °F (540.6 °C).
- The model was re-ran using the temperature data from the tubes expected to cause the most damage.

| Summary of July 20-30 Tube Data |          |          |          |          |          |          |          |          |          |          |          |           |           |           |           |
|---------------------------------|----------|----------|----------|----------|----------|----------|----------|----------|----------|----------|----------|-----------|-----------|-----------|-----------|
| Tube                            | Tube 41A | Tube 41B | Tube 46A | Tube 46B | Tube 51A | Tube 51B | Tube 56A | Tube 56B | Tube 61A | Tube 61B | Tube 66A | Tube 66B  | Tube 70A  | Tube 70B  | Tube 71A  |
| Average Temperature (F)         | 801      | 802      | 804      | 805      | 811      | 814      | 813      | 816      | 810      | 808      | 803      | 809       | 782       | 783       | 804       |
| Maximum Temperature (F)         | 1057     | 1059     | 1090     | 1085     | 1100     | 1099     | 1096     | 1086     | 1089     | 1086     | 1075     | 1074      | 1030      | 1027      | 999       |
| Tube                            | Tube 71B | Tube 76A | Tube 76B | Tube 81A | Tube 81B | Tube 86A | Tube 86B | Tube 91A | Tube 91B | Tube 96A | Tube 96B | Tube 101A | Tube 101B | Tube 105A | Tube 105B |
| Average Temperature (F)         | 804      | 832      | 835      | 845      | 842      | 850      | 853      | 844      | 848      | 837      | 836      | 830       | 833       | 783       | 762       |
| Maximum Temperature (F)         | 1001     | 1054     | 1063     | 1074     | 1071     | 1085     | 1092     | 1074     | 1090     | 1073     | 1074     | 1065      | 1072      | 984       | 962       |

| Summary of September 20-26 Tube Data |          |          |          |          |          |          |          |          |          |          |          |           |           |           |           |
|--------------------------------------|----------|----------|----------|----------|----------|----------|----------|----------|----------|----------|----------|-----------|-----------|-----------|-----------|
| Tube                                 | Tube 41A | Tube 41B | Tube 46A | Tube 46B | Tube 51A | Tube 51B | Tube 56A | Tube 56B | Tube 61A | Tube 61B | Tube 66A | Tube 66B  | Tube 70A  | Tube 70B  | Tube 71A  |
| Average Temperature (F)              | 847      | 849      | 849      | 850      | 853      | 858      | 853      | 857      | 852      | 852      | 851      | 858       | 828       | 831       | 866       |
| Maximum Temperature (F)              | 1026     | 1028     | 1047     | 1043     | 1067     | 1065     | 1090     | 1077     | 1091     | 1089     | 1066     | 1065      | 996       | 989       | 984       |
| Tube                                 | Tube 71B | Tube 76A | Tube 76B | Tube 81A | Tube 81B | Tube 86A | Tube 86B | Tube 91A | Tube 91B | Tube 96A | Tube 96B | Tube 101A | Tube 101B | Tube 105A | Tube 105B |
| Average Temperature (F)              | 866      | 902      | 906      | 914      | 913      | 919      | 923      | 911      | 919      | 905      | 905      | 899       | 904       | 846       | 822       |
| Maximum Temperature (F)              | 984      | 1041     | 1043     | 1048     | 1047     | 1047     | 1052     | 1037     | 1048     | 1043     | 1043     | 1053      | 1063      | 993       | 936       |

# P22 Lifetime Evaluation: Tube 56A

- Number of fatigue cycles in 10 days: 456
  - Let 456 Cycles equal one ten day block.
- ASME BPVC VIII-2 Annex 3F Table 3-F.1: 434 Blocks
  - 11.9 Years until failure
  - Peak Alternating Stress: 203 MPa
- Updated life expectancy represents the minimum known failure time of 10-20 years.
- Possible discrepancy in material model not accurately matching in service component.



# P22 Material

- To validate the material model, data from samples taken from a retired steam header will be evaluated.
- The samples were evaluated at 3 temperatures.
  - 20 °C
  - 300 °C
  - 500 °C
- Each sample was subjected to 50 cycles at the following strains
  - 0.1%, 0.25%, 0.4%, 0.5%, 0.75%, 0.5%, 0.25%



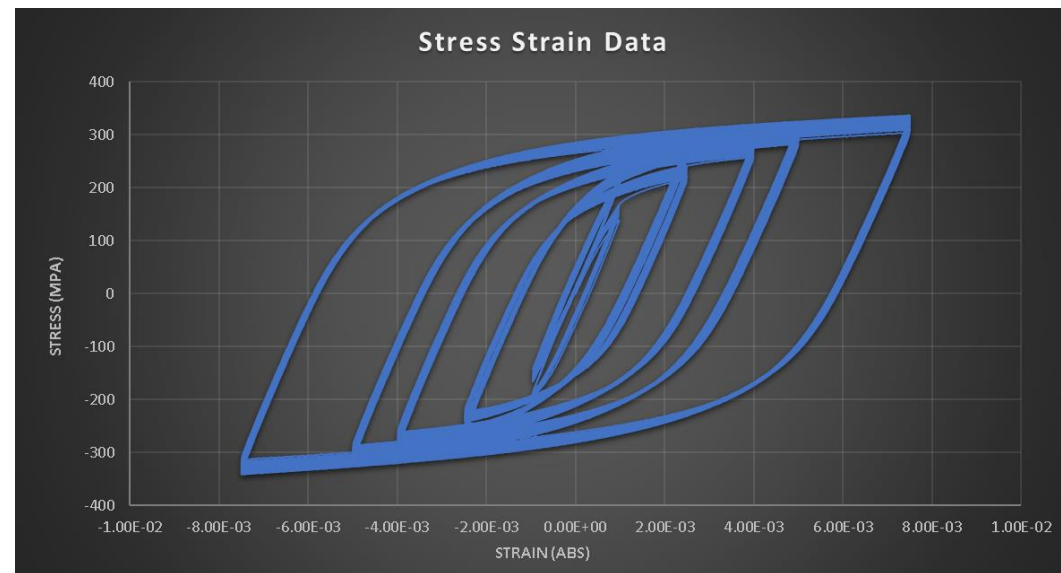
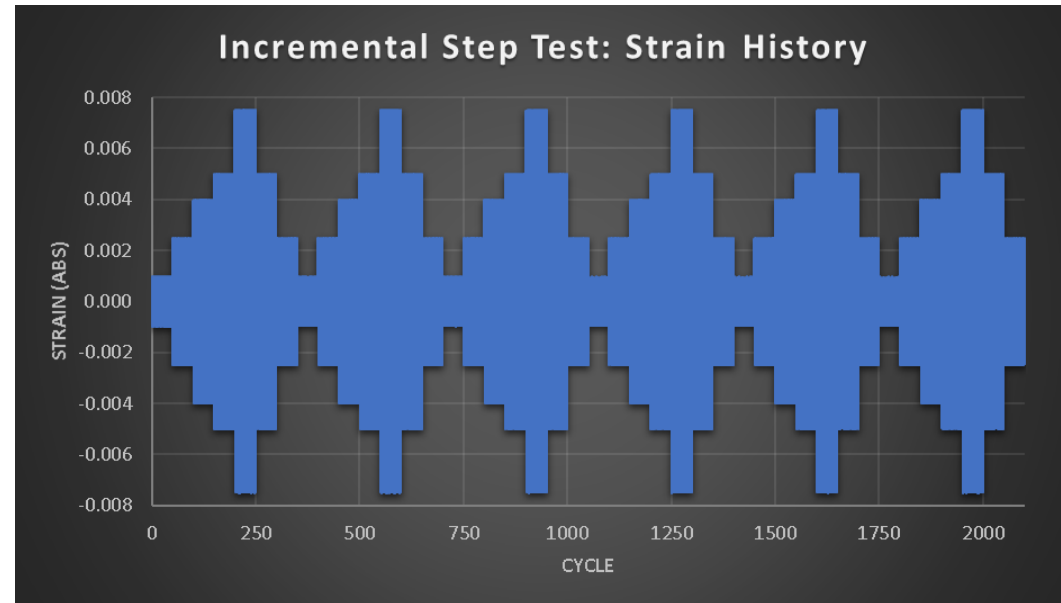
UNC CHARLOTTE

---

*The WILLIAM STATES LEE COLLEGE of ENGINEERING*

# New Material Model Constants

- Stress-Strain data was provided for serviced P22 samples at 3 temperatures.
  - 20 °C
  - 300 °C
  - 500 °C
- Each sample was subjected to 50 cycles at the following strain blocks
  - 0.1%, 0.25%, 0.4%, 0.5%, 0.75%, 0.5%, 0.25%
  - 50 Cycles per block
  - 6 Blocks per sample



# New Material Model Constants

- The desired material model will be a Non-Linear Kinematic Hardening, NLKH, model.
  - The model will not incorporate Isotropic Hardening or Creep effects.
- The provided samples are from a retired unit with an unknown strain history needed to determine Isotropic Hardening material parameters.
- The data provided does not include rate effects required to obtain the Creep material parameters.
- The NLKH constants were found following the procedure outlined in Lemaitre &Chaboche, "Mechanics of Solid Materials ," 1994.



UNC CHARLOTTE

---

*The WILLIAM STATES LEE COLLEGE of ENGINEERING*

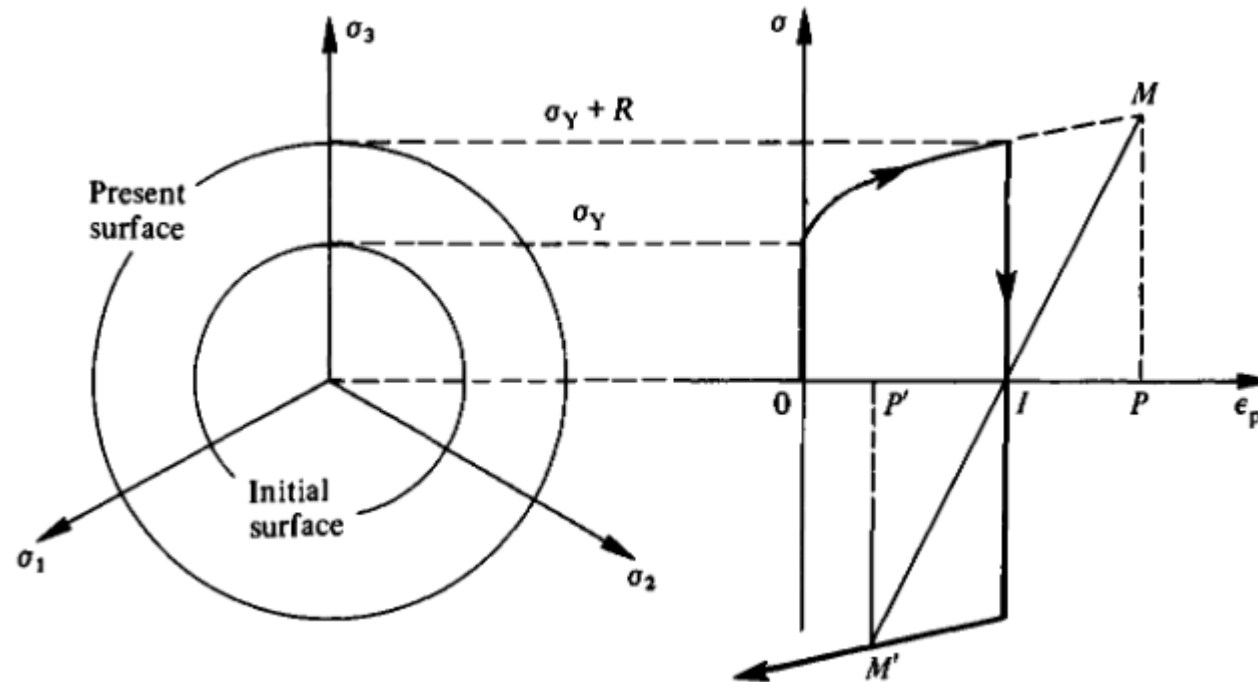
# New Material Model Constants

- Material hardening is generally broken into two categories.
  - Isotropic Hardening
  - Kinematic Hardening
    - Linear
    - Nonlinear
- Isotropic Hardening is used to reflect symmetric increases of the yield surface.
- Kinematic Hardening is used to reflect translations of the yield surface.



# New Material Model Constants

- Isotropic Hardening: Increases yield strength equally in tension and compression.
- The yield function,  $f$ , has the form of  $f = \sigma_{eq} - R - \sigma_y$



UNC CHARLOTTE

The WILLIAM STATES LEE COLLEGE of ENGINEERING

# New Material Model Constants

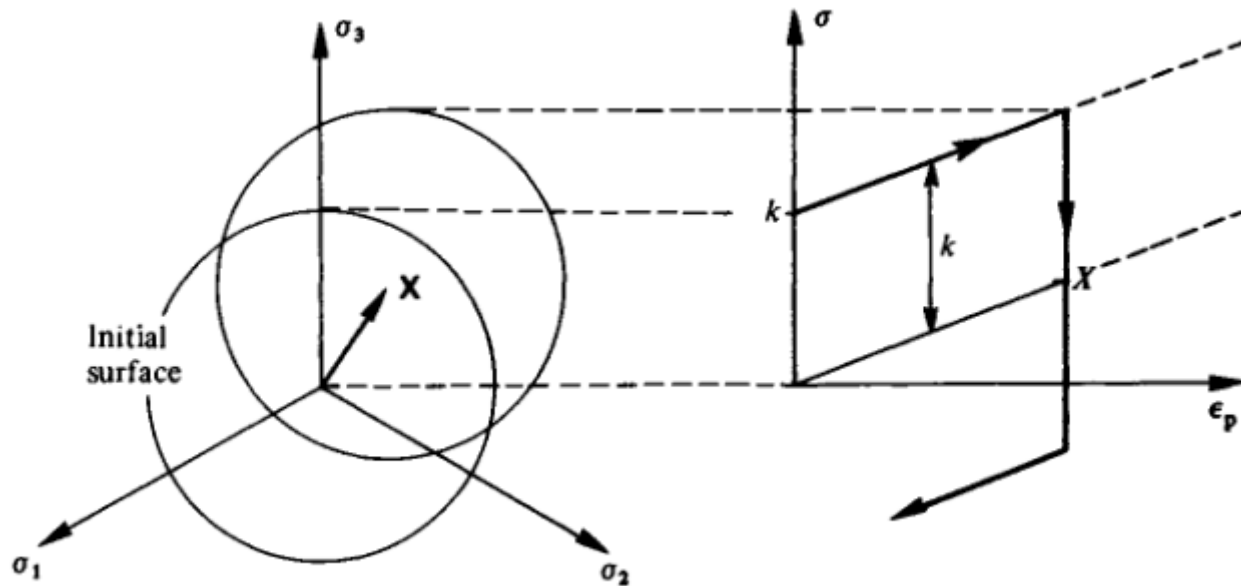
- Under symmetric strain cycles, Isotropic Hardening stabilizes to a set value as the mean stress approaches zero.
- The level of Isotropic Hardening depends on the strain amplitude.
- Therefore, only Kinematic hardening effects are considered when evaluating a stabilized state.
- This can be seen by the definition of the evolution of R.

$$dR = b(Q - R)dp$$



# New Material Model Constants

- Kinematic Hardening: An increase in tensile yield strength reduces the compressive yield strength.
- For Kinematic Hardening, the yield function,  $f$ , has the form of  $f = J_2(\sigma - \chi) - k$

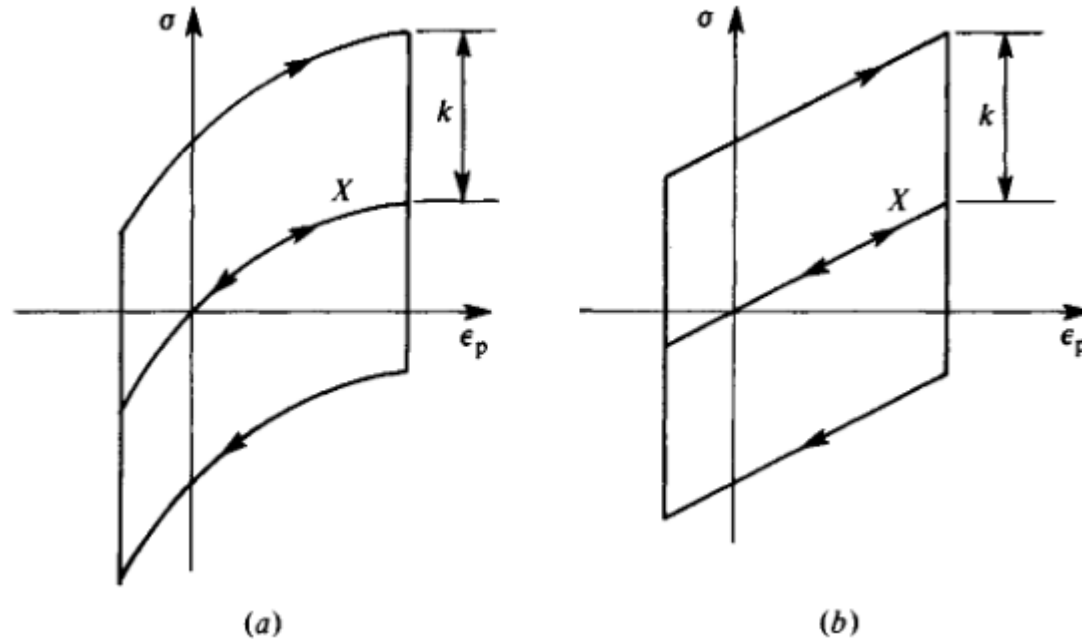


UNC CHARLOTTE

The WILLIAM STATES LEE COLLEGE of ENGINEERING

# New Material Model Constants

- Kinematic Hardening can be represented as linear and nonlinear hardening.
- For linear hardening  $d\chi = C_0 d\varepsilon^p$
- For nonlinear hardening  $d\chi = \frac{2}{3} C d\varepsilon^p - \gamma \chi dp$



UNC CHARLOTTE

The WILLIAM STATES LEE COLLEGE of ENGINEERING



# New Material Model Constants

- Initial constants were found using a single set of coefficients for the NLKH model.
  1. Determine the initial yield stress of the first cycle
  2. Determine the  $\frac{C}{\gamma}$  value as an asymptotic value of  $\Delta\sigma - k$  plotted against  $\Delta\varepsilon$ .
  3. Determine the constants  $C, \gamma$  by fitting the relationship of

$$\frac{\Delta\sigma}{2} - k = \frac{C}{\gamma} \tanh\left(\gamma \frac{\Delta\varepsilon_p}{2}\right)$$

- Note: The modulus was taken as a linear fit of the first 0.00095 strain. The initial yield stress was found as the intersection of the stress strain data and the 0.2% offset modulus.

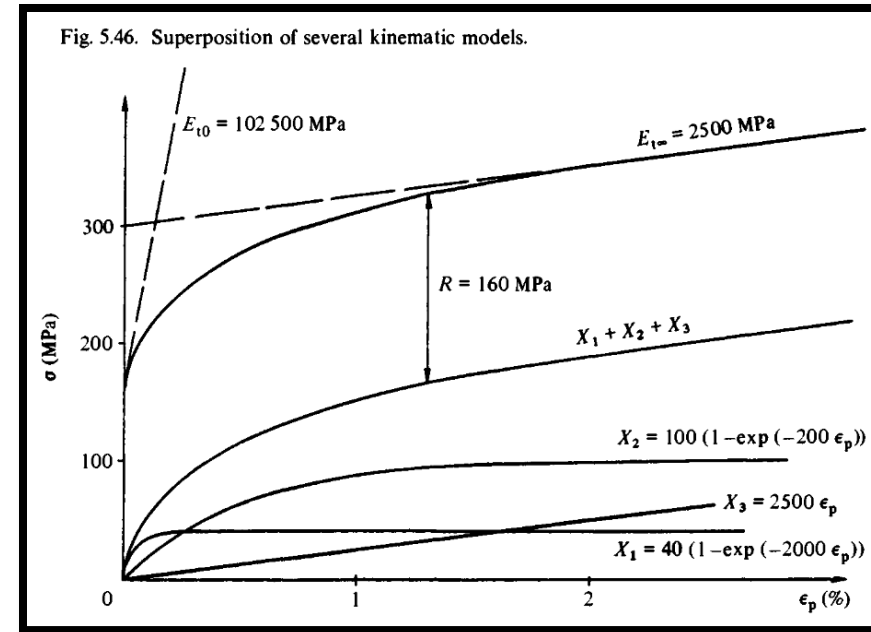


UNC CHARLOTTE

The WILLIAM STATES LEE COLLEGE of ENGINEERING

# New Material Model Constants

- The model was updated to reflect the superposition of multiple NLKH models.
- A python script using the `scipy.optimize.curve_fit()` functionality was used to determine the coefficients  $C, \gamma$
- The model uses Least Square Minimization



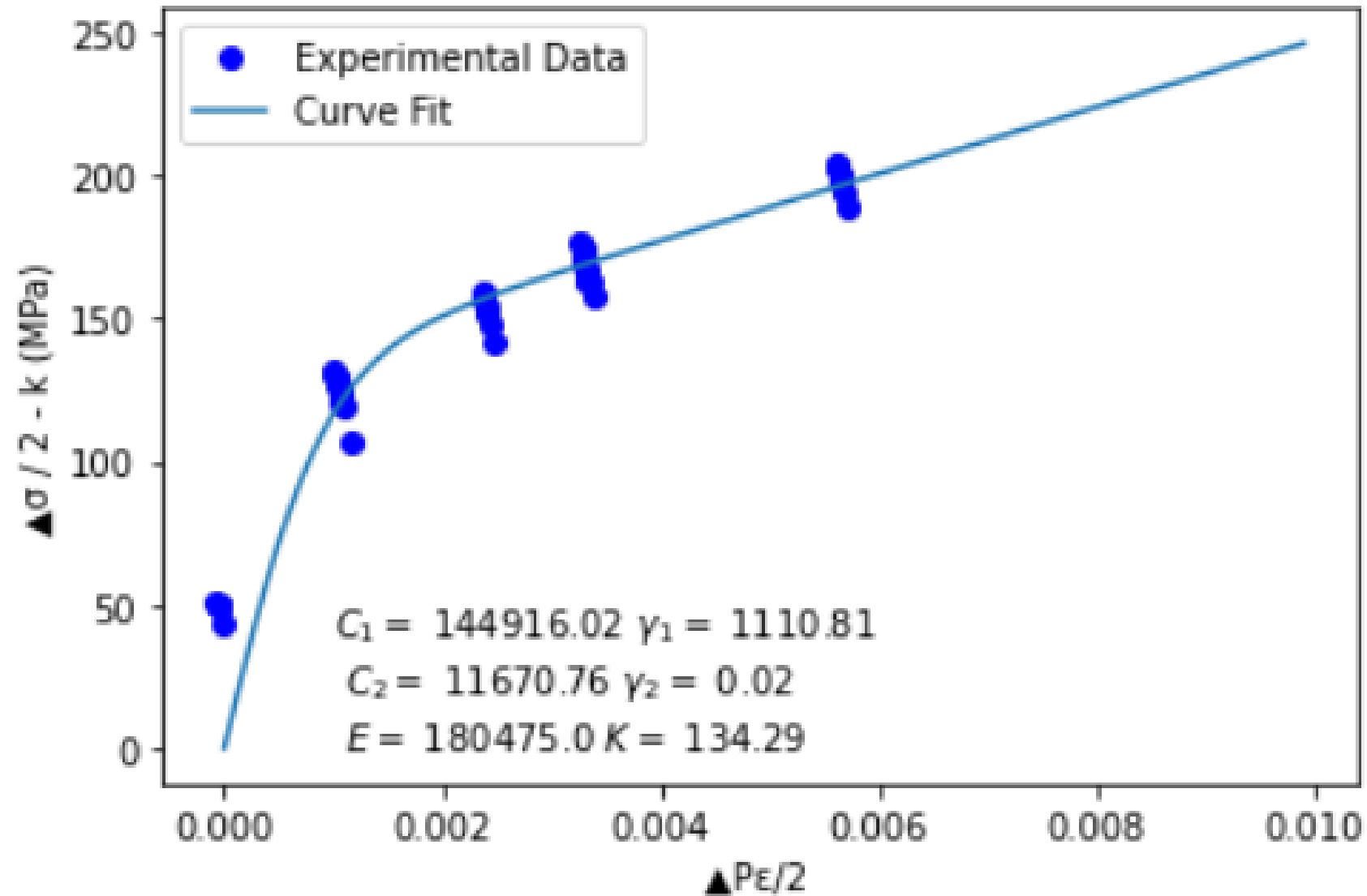
Adapted from [1]

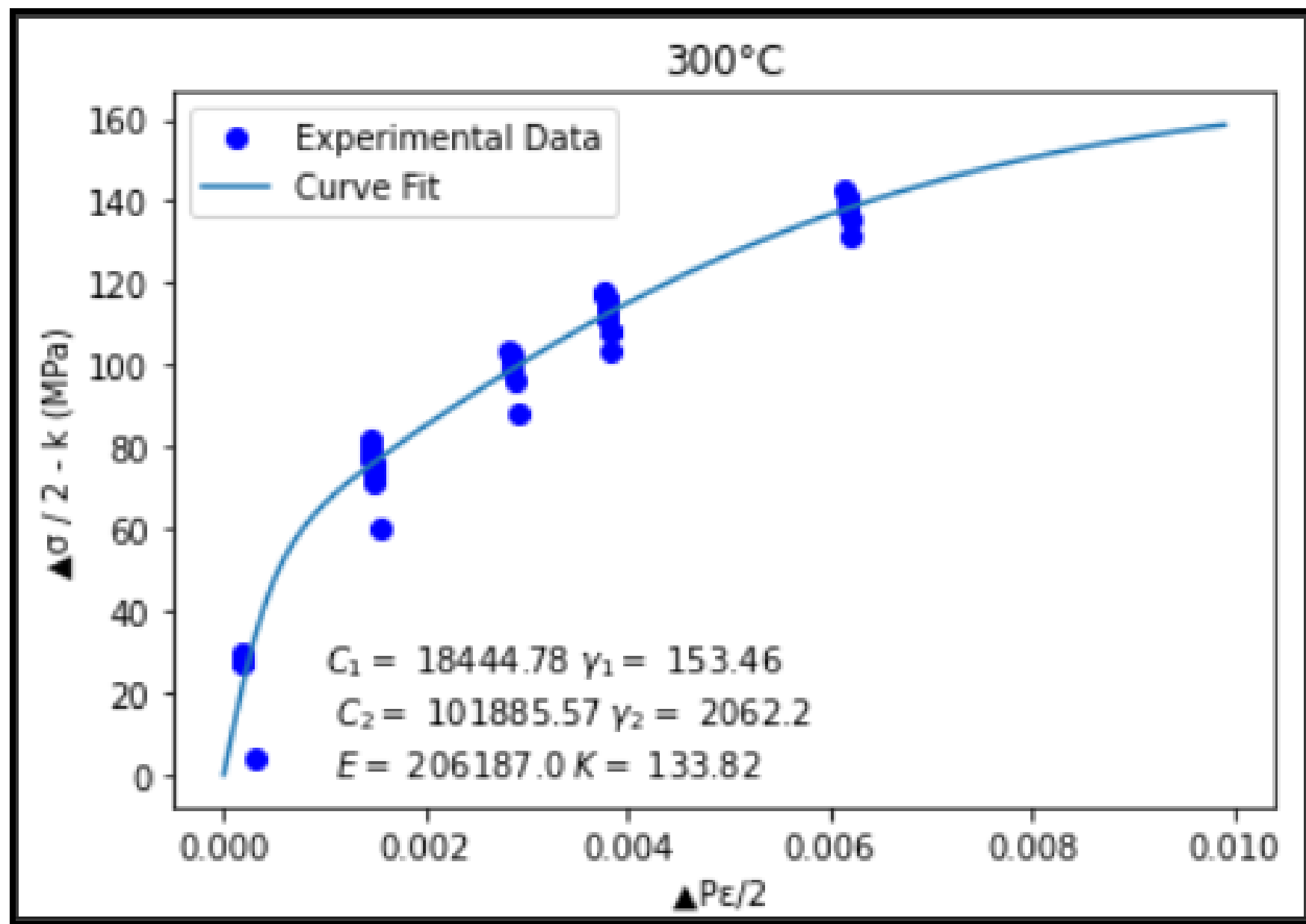


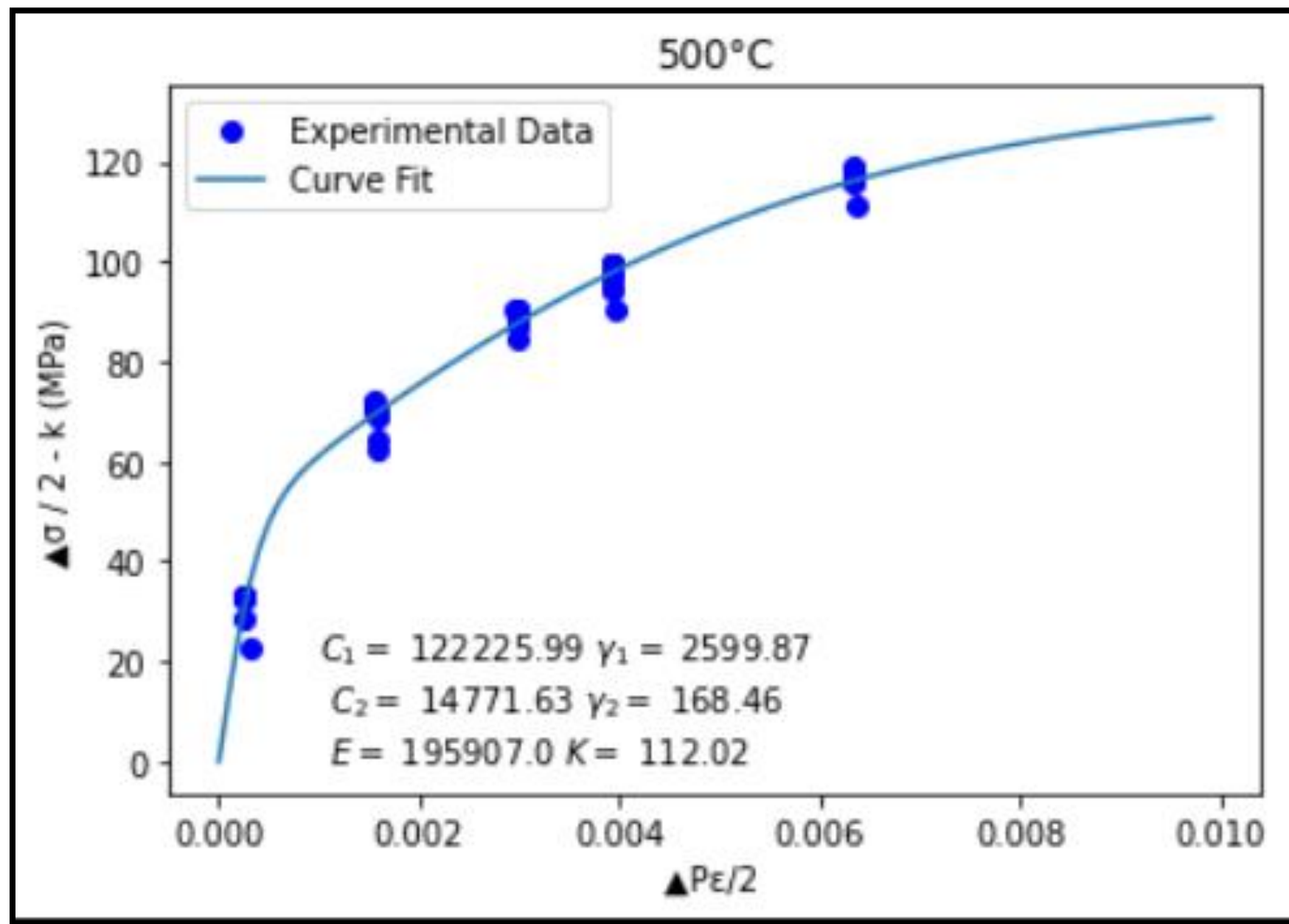
UNC CHARLOTTE

The WILLIAM STATES LEE COLLEGE of ENGINEERING

20°C







# New Material Model Constants

- The updated constants for the NLKH model are shown below.

$$\frac{\Delta\sigma}{2} - k = \frac{C}{\gamma} \tanh\left(\gamma \frac{\Delta\varepsilon_p}{2}\right)$$

| Temperature | E (MPa) | K (MPa) | C <sub>1</sub> | γ <sub>1</sub> | C <sub>2</sub> | γ <sub>2</sub> |
|-------------|---------|---------|----------------|----------------|----------------|----------------|
| 20°C        | 180,475 | 134.29  | 144916.02      | 1,110.81       | 11,670.76      | 0.02           |
| 300°C       | 206,187 | 133.82  | 18,444.78      | 153.46         | 101,885.57     | 2062.2         |
| 500°C       | 195,907 | 112.02  | 122,225.99     | 2,599.87       | 14,771.63      | 168.46         |



# References

- [1] Farragher, T.P., Scully, S., O'Dowd, N.P. and Leen, S.B., 2013. Development of life assessment procedures for power plant headers operated under flexible loading scenarios. *International Journal of Fatigue*, 49, pp.50-61.
- [2] Lemaitre, J. and Chaboche, J.L., 1994. *Mechanics of solid materials*. Cambridge university press.





*Thank you for your participation.*

*Questions?*

---

---



D.O.E. Project  
DE-FE0031747  
Alloy for Enhancement of Operational  
Flexibility of Powerplants